Title
Compositional Constraints are Vital for Atmospheric PM2.5 Source Attribution over India

Journal
ACS Earth and Space Chemistry, 6(10)

ISSN
2472-3452

Authors
Pai, Sidhant J
Heald, Colette L
Coe, Hugh
et al.

Publication Date
2022-10-20

DOI
10.1021/acsearthspacechem.2c00150

Peer reviewed

ACS EARTH AND SPACE CHEMISTRY

http://pubs.acs.org/journal/aesccq

Article

Compositional Constraints are Vital for Atmospheric $PM_{2.5}$ Source Attribution over India

Sidhant J. Pai,* Colette L. Heald,* Hugh Coe, James Brooks, Mark W. Shephard, Enrico Dammers, Joshua S. Apte, Gan Luo, Fangqun Yu, Christopher D. Holmes, Chandra Venkataraman, Pankaj Sadavarte, and Kushal Tibrewal

Cite This: *ACS Earth Space Chem.* 2022, 6, 2432–2445

Read Online

ACCESS | Metrics & More | Article Recommendations | Supporting Information

ABSTRACT: India experiences some of the highest levels of ambient $PM_{2.5}$ aerosol pollution in the world. However, due to the historical dearth of in situ measurements, chemical transport models that are often used to estimate $PM_{2.5}$ exposure over the region are rarely evaluated. Here, we conduct a novel model comparison with speciated airborne measurements of fine aerosol, revealing large biases in the ammonium and nitrate simulations. To address this, we incorporate process-level changes to the model and use satellite observations from the Cross-track Infrared Sounder (CrIS) and the TROPOspheric Monitoring Instrument (TROPOMI) to constrain ammonia and nitrogen oxide emissions. The resulting simulation demonstrates significantly lower bias ($NMB_{Modified}$: 0.19; NMB_{Base}: 0.61) when validated against the airborne aerosol measurements, particularly for the nitrate ($NMB_{Modified}$: 0.08; NMB_{Base}: 1.64) and ammonium simulation ($NMB_{Modified}$: 0.49; NMB_{Base}: 0.90). We use this validated simulation to estimate a population-weighted annual $PM_{2.5}$ exposure of 61.4 $\mu g\ m^{-3}$, with the RCO (residential, commercial, and other) and energy sectors contributing 21% and 19%, respectively, resulting in an estimated 961,000 annual $PM_{2.5}$-attributable deaths. Regional exposure and sectoral source contributions differ meaningfully in the improved simulation (compared to the baseline simulation). Our work highlights the critical role of speciated observational constraints in developing accurate model-based $PM_{2.5}$ aerosol source attribution for health assessments and air quality management in India.

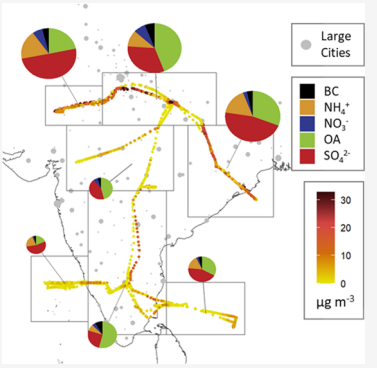

KEYWORDS: *air pollution, speciated aerosols, $PM_{2.5}$ source attribution, satellite measurements, India*

1. INTRODUCTION

India has some of the highest ambient air pollution levels in the world,[1,2] with studies estimating that elevated $PM_{2.5}$ aerosol in the country contributes to between 0.4 and 1.1 million annual $PM_{2.5}$-attributable deaths.[1−7] High aerosol concentrations have also been shown to impact regional crop yields[8,9] and disrupt seasonal rainfall over the subcontinent.[10,11] Aerosol pollution has severely impacted economic productivity and quality of life in India, resulting in estimated annual losses of $505 billion and $55 billion in welfare and forgone labor output.[12] Economic development is predicted to drive a substantial increase in pollution in India over the coming decades.[1,13] However, as air quality management becomes more stringent, the emissions of certain types of pollutants are also expected to decrease.[14] These trends are expected to result in a meaningful shift in source-sector emission profiles, amplifying the need for targeted air quality management policies based on credible models that accurately reflect the regionally specific sources and chemical composition of fine aerosol.[15]

$PM_{2.5}$ particles are produced from a variety of sources. Primary aerosols, like mineral dust and black carbon soot, are emitted directly into the atmosphere, usually via mechanical processes. In contrast, secondary aerosols are formed via chemical and thermodynamic interactions in the atmosphere. Recent work has indicated that a large fraction of the regional $PM_{2.5}$ burden in India is secondary in nature, even in urban cities like Delhi.[16−19] Regional chemical transport models (CTMs) thus play a central role in estimating the sources and fates of these air pollutants. Numerous studies rely on CTM output to explore the importance of different emission sources and determine the magnitude of health outcomes from $PM_{2.5}$ exposure.[1,3,4,20−24] In aggregate, these studies help form the basis for air quality management strategies in the region.[25] However, the complexities associated with the various processes that dictate aerosol concentrations make accurately simulating the mass and composition of $PM_{2.5}$ very challenging. This is compounded by the large spread in

Received: May 17, 2022
Revised: July 23, 2022
Accepted: July 25, 2022
Published: September 16, 2022

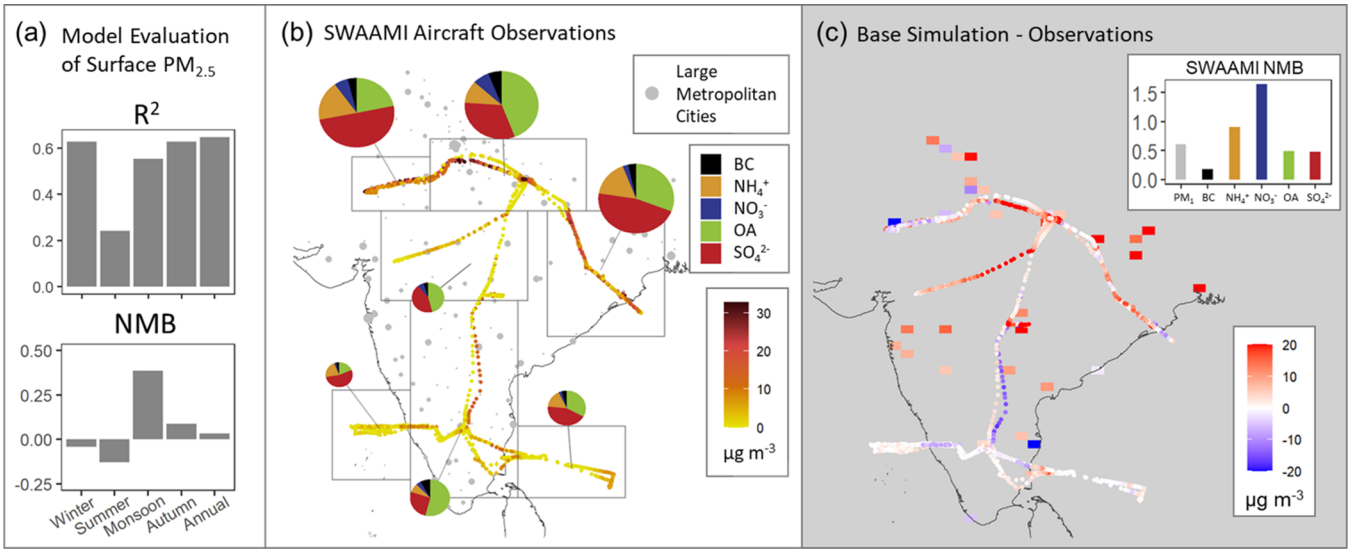

Figure 1. (a) Seasonal comparison of model skill for the 'Base' simulation relative to surface $PM_{2.5}$ observations at 123 sites in India in 2017 using the coefficient of determination (R^2) and the normalized mean bias (NMB). Seasons are defined as winter (DJF), summer (MAM), monsoon (JJA) and autumn (SON). (b) Observed fine aerosol concentrations along the SWAAMI flight tracks in June and July 2016. The dataset is divided into individual regions (outlined in gray boxes) with the pie charts representing the fractional contribution of individual species to the total aerosol burden within that region. (c) Difference in the modeled and observed fine aerosol concentrations for the Base simulation compared to both the airborne (circles) and surface (rectangles) observations during the monsoon period (June to July 2016). The subpanel shows the NMB values for individual model aerosol species and total fine aerosol less than 1 μm in diameter (PM_1, defined here as the sum of the individual aerosol species) compared to the airborne measurements. Refer to the Supporting Information for information on the SWAAMI instrumentation and model comparison.

model configurations used across different studies, with simulations varying significantly in their treatment of emissions, chemistry, transport, and loss processes.

The uncertainties stemming from different model configurations have been exacerbated by the historical dearth of chemically speciated aerosol measurements across most of the country. India continues to have a much lower density of surface $PM_{2.5}$ monitors compared to other highly populated countries,[26,27] making it challenging to validate aerosol simulations, despite evidence of model bias.[28] To account for these deviations, satellite aerosol optical depth (AOD) retrievals have been used in conjunction with CTMs and limited surface data to scale regional aerosol simulations.[29−31] Previous studies, such as the Global Burden of Disease (GBD) MAPS working group assessment, have used this approach to estimate population exposures, health outcomes, and aerosol source attributions over India.[1] While these methods have been shown to reduce the overall bias in simulated $PM_{2.5}$ concentrations relative to surface observations, the scaling approach does not identify or correct the underlying biases in model aerosol composition, and the resulting source attributions thus retain their relative biases.

The goal of this study is to go beyond previous work by characterizing and remedying underlying model biases prior to conducting a $PM_{2.5}$ source apportionment and mortality assessment over the Indian subcontinent. This study leverages a suite of novel measurements and explores the key role of speciated aerosol constraints. The resulting analysis represents a comprehensive framework for source-segregated premature mortality assessments associated with $PM_{2.5}$.

2. METHODS

2.1. Default Model Configuration. We use the GEOS-Chem CTM[32] (www.geos-chem.org) to simulate aerosol mass concentrations over the Indian subcontinent, performing a series of simulations ranging from 2016 to 2019. All simulations are performed using the GEOS-Chem model version 12.1.1 (https://doi.org/10.5281/zenodo.2249246), using a custom-nested grid at a horizontal resolution of 0.5° × 0.625° with 47 vertical hybrid-sigma levels. The nested simulations (60°E to 105°E; 0° to 44°N) use boundary conditions from a 2° × 2.5° global run and are driven using the MERRA-2 assimilated meteorological product from the NASA Global Modeling and Assimilation Office (GMAO), with a transport time step of 10 min as recommended by Philip et al.[33] The model uses a coupled treatment of HO_x-NO_x-VOC-O_3 chemistry[34−36] with integrated peroxyacetyl nitrate and halogen chemistry[37,38] and simulates important aerosol species including sulfate (SO_4^{2-}), nitrate (NO_3^-), ammonium (NH_4^+) (SNA),[39] sea-salt,[40] black carbon (BC),[41,42] organic aerosol (OA),[43] and mineral dust.[44,45] SNA thermodynamics are described using the ISORROPIA II model.[46] Black carbon is modeled as two separate hydrophobic and hydrophilic species, with the hydrophobic BC aging to hydrophilic BC in the atmosphere, with a lifetime of 1.2 days.[41] Primary organic aerosol (POA) is similarly emitted to both hydrophobic and hydrophilic species, with hydrophobic POA aging to hydrophilic POA with an atmospheric lifetime of 1.2 days.[47,48] OA aerosol mass is estimated using an OA:OC ratio of 1.4 for primary emissions and an OA:OC ratio of 2.1 for aged organic aerosol.[43] Model aerosol optical depth (AOD) is calculated using RH-dependent aerosol optical properties.[45,49] Aerosol and gas dry deposition loss to surfaces is simulated using a resistor-in-series scheme.[50,51] Wet deposition occurs via scavenging by rainfall and moist convective cloud updrafts.[52−54]

Model comparisons with aircraft observations are conducted by sampling the simulation at the spatial and temporal

https://doi.org/10.1021/acsearthspacechem.2c00150
ACS Earth Space Chem. 2022, 6, 2432−2445

coordinates consistent with the observational data. We filter the observations to remove concentrations over the 97th percentile for each flight, to limit the impact of localized pollutant plumes that cannot be reproduced by an Eulerian model.[55] The model does not explicitly simulate particle size, but assumes a standard log-normal distribution. PM_1 model aerosol mass can thus be estimated, since the fractional mass of simulated dry BC, OA, and SNA aerosols above 1 μm in diameter is negligible. We do not include fine dust and sea-salt aerosol from the model in the PM_1 comparisons since these species were not measured during the aircraft campaign (Section 2.3; Figure 1). However, we include all the above species in the $PM_{2.5}$ comparisons with the surface network, after applying the appropriate growth factors at 35% relative humidity[49,56,57] and sub-sampling the model dust and sea-salt aerosol mass to only include particles below 2.5 μm in diameter. We conduct a year-long simulation for 2016 for the main analysis, and also run simulations for 2017−2019 to conduct comparisons with surface observations and TROPOMI satellite measurements (Sections 2.4 and 2.5). All model simulations were spun-up for 3−6 months and use time-appropriate dependencies (emissions, meteorology, etc.).

2.2. Model Emissions. Global anthropogenic emissions in the baseline (Base) model follow the Community Emissions Data System (CEDS) inventory v2018−08.[58] Nitrogen oxides are also emitted from lightning,[59,60] soil,[61] and ship[62] sources. Anthropogenic dust emissions from fugitive sources are also included.[63] Biogenic emissions for isoprene and terpene species in GEOS-Chem are based on the coupled ecosystem emissions model MEGAN (Model of Emissions of Gases and Aerosols from Nature) v2.1.[64] Year-specific pyrogenic emissions are simulated at a 3 h resolution from the GFED4s satellite-derived global fire emissions database.[65] To compare the differences in emission estimates across various studies, we perform multiple nested simulations using five different monthly varying anthropogenic inventories: CEDS v2018-08,[58] MIX v1.1,[66] SMoG-India v0,[67,68] ECLIPSE v5a,[69] and EDGAR v4.3.[70] The base inventory (CEDS) extends natively to the years simulated in this study, but the other inventories do not. When this is the case, we use emissions from the closest year recorded in the inventory. Sensitivity simulations are also conducted using the GFAS v1.2,[71] FINN v1.5,[72] and QFED v2.4[73] fire inventories.

2.3. Airborne Aerosol Mass Measurements. The South West Asian Aerosol Monsoon Interactions (SWAAMI) aircraft campaign consists of 17 flights from June to July 2016 over the Indian subcontinent.[74] Speciated submicron non-refractory dry aerosol mass concentrations of both organic and inorganic species were measured on-board the aircraft using a compact time-of-flight aerosol mass spectrometer (AMS),[75] with an estimated uncertainty of approximately 34−38% depending on the species.[76] Black carbon mass concentrations were measured using a Single Particle Soot Photometer (SP2),[77] with an uncertainty of approximately 30%.[74]

2.4. Satellite Observations. We use NASA satellite measurements of Aerosol Optical Depth (AOD) from the Moderate Resolution Imaging Spectroradiometer (MODIS) instrument on board the TERRA and AQUA platforms to analyze daily aerosol AOD[78] over the Indian subcontinent for the year 2016. We use 10 years of monthly Level 3 gridded data from the Cloud-Aerosol Lidar with Orthogonal Polarization (CALIOP) instrument[79,80] aboard the Cloud-Aerosol Lidar and Infrared Pathfinder Satellite Observation (CALIPSO) satellite to estimate the fractional contribution of dust over the Indian subcontinent during the monsoon season. We use satellite column retrievals of NH_3 and NO_2 from the Cross-track Infrared Sounder[81−83] (CrIS, aboard Suomi-NPP) and TROPOspheric Monitoring Instrument[84,85] (TROPOMI, aboard Sentinel-5 Precursor), respectively, to generate spatially varying gridded monthly scaling factors, based primarily on the ratio of model and satellite column concentrations, that are then applied to the default model emissions. TROPOMI-derived scale factors are based on model simulations conducted in 2018−2019, since measurements are unavailable for 2016. Additional details on the satellite products, averaging kernel adjustments, and a comparison of TROPOMI retrievals with NO_2 measurements from the Ozone Monitoring Instrument (OMI) are provided in the Supporting Information.

2.5. $PM_{2.5}$ Surface Measurements and ACSM Observations. To evaluate model output at the surface, we use $PM_{2.5}$ measurements made in 2017 from government monitoring sites across 123 different locations in 52 cities, acquired using the OpenAQ (www.openaq.org) cloud repository.[86−88] $PM_{2.5}$ concentrations are measured using beta ray attenuation monitors specified at 35% relative humidity.[57,89] Uncertainties were not defined at the individual locations and can be expected to have a lower-bound of 10%[90] but are likely much higher.[27] These measurements are filtered to only include positive non-zero observations, so as to disregard non-physical values resulting from the lack of standardized reporting across different sites. Measurements above 500 $\mu g\ m^{-3}$ were also filtered out to limit the impact of large sub-grid plumes. These values were then averaged over the model grid resolution over a monthly period to enable a comparison with model output.

In addition, we use speciated aerosol measurements[91] made in 2017 from an Aerosol Chemical Speciation Monitor (ACSM)[92] located at the Delhi supersite location[16] to conduct a limited evaluation of model performance at that one location. The ACSM measurements have an uncertainty of approximately 20−25%.[16]

2.6. Pollution-Attributable Mortality Estimates. We use an integrated exposure-response (IER) model, following the GBD MAPS analysis over India[1] and Burnett et al.,[93] to relate $PM_{2.5}$ exposure to an increased risk in mortality from lower respiratory infections, chronic obstructive pulmonary disease, ischemic heart disease, lung cancer, and stroke using a relative risk (RR) calculation:[1,3,93,94]

$$RR = 1 + \alpha(1 - e^{-\beta(PM_{conc} - Z_{cf})^{\delta}}) \quad (1)$$

The α, β, Z_{cf}, and δ parameters for each disease category are derived from Monte Carlo simulations conducted by Burnett et al.[93] and are available at http://ghdx.healthdata.org/sites/default/files/record-attached-files/IHME_CRCurve_parameters.csv. We determine the mean RR while also calculating the 95th percentile confidence interval using these coefficients to provide an uncertainty range. This interval does not include uncertainty in the model $PM_{2.5}$ estimate, baseline mortality rates, or population distribution. The number of attributable deaths from all disease categories due to $PM_{2.5}$ exposure is calculated using the following relationship:

https://doi.org/10.1021/acsearthspacechem.2c00150
ACS Earth Space Chem. 2022, 6, 2432−2445

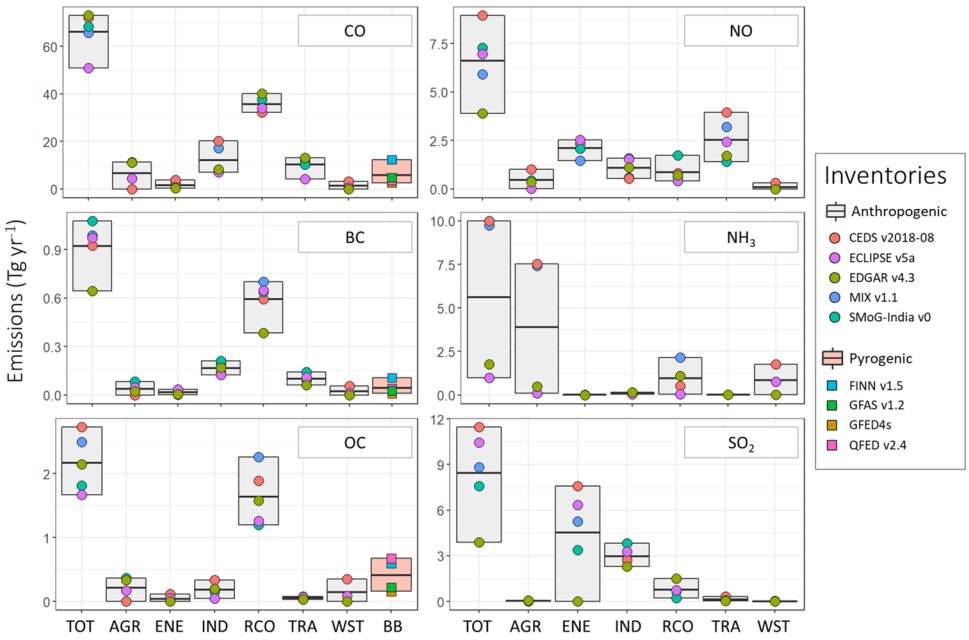

Figure 2. Box plots describing the spread in 2016 emission estimates for India, shown by sector (in Tg year^{-1}). The sectoral emissions for each individual emission inventory are illustrated as filled circles when available. Pyrogenic emissions are based on a 12-year average obtained from Carter et al.[99] Sectors are abbreviated as follows: total (TOT), agricultural (AGR), energy (ENE), industrial (IND), residential, commercial, and other (RCO), transport (TRA), and waste (WST). See the Methods section for details on the emission inventories.

$$PM_{2.5}\ \text{attributable deaths} = \sum \frac{RR_{disease} - 1}{RR_{disease}} \times BMR_{disease} \times POP \quad (2)$$

Age-specific and state-specific baseline mortality rates (BMR) across India are aggregated from the State of Global Air Portal.[95] Gridded population (POP) data is derived from the Gridded Population of the World (GPW v4) dataset[96] based on the 2011 national census[97] and scaled using national-level 2016 population estimates from the World Bank.[98] This dataset is also used to estimate population-weighted annual $PM_{2.5}$ exposure across different states (Table S1). An alternative health-impact analysis following the methodology described by McDuffie et al.,[5] which uses the 2019 GBD concentration-response functions and national-level mortality and exposure data, is also conducted and detailed in the Supporting Information.

2.7. Sectoral Pollutant Source Attribution. To estimate the relative importance of different sectoral emission sources, sensitivity simulations are conducted via multiple model runs that iteratively remove individual sectoral emissions across all pollutant and precursor species within India. Sectoral source influence is then determined based on subtracting regionally averaged $PM_{2.5}$ concentrations from the corresponding values in the baseline simulation. Attributable deaths are estimated by linearly apportioning the total disease burden based on the fractional contribution of an individual sector to the population-weighed $PM_{2.5}$ exposure in each grid box. When aggregated across all sectors, individual contributions account for around 113% of the total population-weighted $PM_{2.5}$ exposure, indicating the general robustness of this approach despite the non-linear response in aerosol burdens from changing emissions. Secondary species like nitrate display a stronger non-linear response. Refer to Tables S2 and S3 for more information.

3. RESULTS AND DISCUSSION

3.1. Assessing Model Fidelity. A comparison of annual average GEOS-Chem CTM surface $PM_{2.5}$ concentrations for 2017 with total $PM_{2.5}$ mass observations from 123 different surface monitoring sites in India (Figure 1a) suggests that the model is reasonably skilled at capturing total $PM_{2.5}$ magnitude and variability across the region (R^2 of 0.65 and normalized mean bias (NMB) of 0.03). However, a seasonal comparison of the same data (Figure 1a) indicates that the model performance is significantly degraded in the summer and monsoon seasons, pointing to underlying mechanistic deficiencies.

To evaluate the model's ability to capture individual aerosol species, we leverage observations from the 2016 SWAAMI airborne campaign,[74] the first real-time speciated airborne measurements of fine submicron (PM_1) dry aerosol mass over India (Figure 1b). The observed aerosol mass burden is dominated by organic and sulfate species, with large localized contributions from ammonium (NH_4^+) and nitrate (NO_3^-) aerosol. Overall, the model overestimates PM_1 aerosol concentrations in the north and underestimates concentrations in the south and northwest during the flight campaign period (monsoon season: JJA). The Base model simulates 48% of the observed variability in the airborne fine aerosol concentrations, with a somewhat high aggregate bias (NMB: 0.61) (Figure 1c). Model comparisons with the observed BC, OA, and SO_4^{2-} are generally robust and consistent with the performance seen in global comparisons.[43] However, this evaluation reveals substantial biases in the simulation of ammonium and nitrate aerosol, with nitrate aerosol in particular demonstrating an extremely high model overestimate (NMB: 1.64). A seasonal comparison with speciated fine particulate concentrations over a single surface site in Delhi (refer to the Supporting Information) confirms the large discrepancies in simulated nitrate (NMB: 1.04). Thus, while the standard simulation generally captures the variability in the aggregate fine aerosol

https://doi.org/10.1021/acsearthspacechem.2c00150
ACS Earth Space Chem. 2022, 6, 2432−2445

mass during SWAAMI, an analysis of the individual species reveals large deviations in model fidelity, highlighting the inadequacy of evaluating the model with total PM_1 or $PM_{2.5}$ mass constraints alone. Furthermore, the large, pervasive biases in the ammonium and nitrate simulations demonstrate the challenge and risks associated with using the Base model configuration for assessing speciated pollutant exposures and source attributions.

Coincident comparison of the simulated aerosol optical depth (AOD) against MODIS satellite observations during the 2016 monsoon season indicates that model AOD is biased low in the north and west (Figure S1), in contrast with the spatial bias in fine aerosol concentrations measured during the SWAAMI airborne campaign (Figure 1c). An analysis of 10 years of LIDAR-based AOD data from the CALIOP instrument suggests that dust accounts for a major fraction of the AOD column over northern India during the monsoons (Figure S1), consistent with a previous study that demonstrated that the regional dust source is biased in the model.[63] This highlights the limitations of relying exclusively on satellite AOD products, which are inherently unspeciated, to constrain speciated $PM_{2.5}$ CTM simulations over the Indian subcontinent.

3.2. Emission Uncertainties. Emissions are a key uncertainty in characterizing aerosol pollution over India.[100] Figure 2 highlights the variance in sectoral emissions estimates across different species for five different emissions inventories commonly used by CTMs to simulate aerosols in the region (spatial patterns are shown in Figure S2). While these inventories vary in terms of sectoral disaggregation and the years that they represent (spanning emission years 2010−2015), there is a particularly wide spread in emission estimates for ammonia (NH_3; factor of 10.2) and nitrogen oxides (NO_x; factor of 2.3), important precursors for ammonium and nitrate aerosol. The large uncertainties in emissions estimates, and the wide variation among the resulting inventories, are important drivers of model uncertainty when conducting exposure estimation and sectoral apportionment, and likely contribute to the lack of model fidelity in simulating ammonium and nitrate during SWAAMI.

3.3. Improving the Model Simulation. Our comparison of the baseline simulation with the airborne AMS data provides insight into species-specific model biases and enables us to identify and target the most beneficial avenues for model improvement. In this instance, the compositional analysis directs us to improve the nitrate simulation over the region. We begin by updating the model dry deposition scheme,[101] with the goal of improving HNO_3 dry deposition (a nitrate precursor species). We also incorporate modifications to the model treatment of dinitrogen pentoxide (N_2O_5) uptake onto aerosol, based on a recent empirical parameterization of the process, as well as modifications to constrain the N_2O_5 uptake efficiency and the $ClNO_2$ production yield.[102,103] Given the high burden of dust in the region, we also configure the model to include an explicit mechanism for acidic uptake onto dust particles.[104] The above updates were found to have a modest but directionally accurate impact on the simulation, resulting in a decrease in model bias of around 10%.

Given that the SWAAMI campaign largely sampled monsoon conditions, we expect the model treatment of wet scavenging to play an important role in determining model fidelity. We thus incorporate a number of modifications to the wet deposition scheme (described by Luo et al.[105]) that replace the constant in-cloud condensation water (ICCW) assumed in GEOS-Chem with a variable value derived from the assimilated meteorology product. We also implement an empirical washout rate for nitric acid from the same study, which affects the below-cloud scavenging rate. These changes result in a substantial increase in depositional losses relative to the Base simulation. We note that the above modifications to the wet deposition scheme also impact a variety of other aerosol and precursor burdens (e.g., dust and organic aerosol).

To constrain the large uncertainties in the nitrate and ammonium precursor emissions (Section 3.2), and to better capture their spatial and temporal distributions, we also generate emission masks based on monthly averaged model-satellite comparisons for NO_2 and NH_3 by estimating the relative ratio in column concentrations and deriving a scale factor for each grid box (refer to the Supporting Information for more details on averaging kernel and air mass factor application). The comparisons were conducted at a model grid resolution of $0.5° \times 0.625°$, regridded to a CEDS emission inventory resolution of $0.5° \times 0.5$, and then interpolated across the region. Scaling factors were bound between 0.5 and 2 to prevent localized plume effects and to limit any excess deviation from the original emissions estimate. To account for the limited availability of CrIS observations during the monsoon season, the available gridded scaling factors for NH_3 were averaged across 14 Agro-Climatic zones (refer to the Supporting Information) for the months of June and July. The resulting monthly emission masks for NH_3 and NO_x were then applied consistently across the 2016−2017 model simulation years. This approach provides only a coarse constraint on regional emissions. A more robust inverse modeling effort could help separate emissions sectors and geographical contributions at a greater precision, but would require an additional suite of novel observational constraints and a different modeling paradigm (i.e., an adjoint model; e.g., Choi et al.).[106]

3.4. Modified Model Performance. The adjustments and modifications described in Section 3.4 result in a large increase in aerosol precursor removal via wet deposition, with the total deposition of NH_3 and HNO_3 over India increasing by 4% and 62%, respectively, relative to the Base simulation. When comparing model concentrations of NO_2 and NH_3 with the satellite retrievals (described in Section 3.3), we find that the difference between monthly mean satellite retrievals and simulated column concentrations (from the mechanistically adjusted simulation) can be substantial, exceeding a factor of 2 in 71% and 15% of cases for NH_3 and NO_x, respectively. The satellite-based scaling increases annual national NH_3 and NO_x emissions by 26% and 32%, respectively, with important seasonal differences (Figures S3 and S4). Recent work has also indicated that TROPOMI column retrievals are biased low over polluted regions,[107] suggesting that the NO_x scaling factors in this study might be conservative.

Overall, the refined simulation (referred to here as the 'Modified' simulation) substantially outperforms the Base simulation when evaluated against the SWAAMI campaign (Figure 3), with a significantly lower normalized mean bias (Base: 0.61; Modified: 0.19) and a slightly improved R^2 (Base: 0.48; Modified: 0.51) across the total aerosol PM_1 mass. The simulation of individual species is also improved for the monsoon season. In particular, the bias in the nitrate simulation is drastically decreased (NMB Base: 1.64; Modified: 0.08), although the simulation remains unable to capture the

https://doi.org/10.1021/acsearthspacechem.2c00150
ACS Earth Space Chem. 2022, 6, 2432−2445

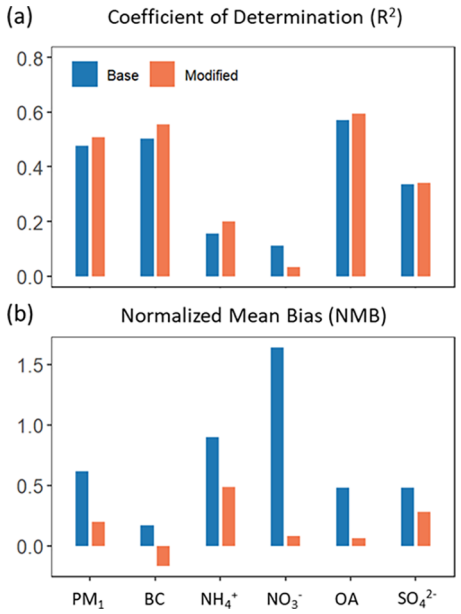

Figure 3. Comparison of model skill between the Base (blue) and Modified (orange) simulations when compared to the aircraft AMS observations from the SWAMMI airborne campaign in 2016 (see Figure 1b) using (a) the coefficient of determination and (b) the normalized mean bias.

spatial variability in the nitrate observations (Figure 3a). Figure S5 shows that the vertical profile is also better represented in the Modified simulation.

Revisiting the $PM_{2.5}$ comparisons shown in Figure 1a (Figures S6 and S7), the Modified simulation modestly improves the Base model's ability to capture the observed annual variability (R^2 – Base: 0.65, Modified: 0.68) but results in a significant reduction in bias during the monsoon season (NMB – Base: 0.38, Modified: 0.02), providing more independent validation of the modifications made to the Base simulation. When compared to speciated measurements of PM_1 aerosol mass from an urban surface monitoring location in Delhi, the Modified simulation significantly reduces the Base model overestimate of nitrate aerosol (NMB – Base: 1.04, Modified: 0.60) and improves the ammonium simulation for all seasons except the winter (Figure S8). Despite the substantial improvements in the simulation of individual species, the sulfate simulation remains biased high when compared to the SWAAMI dataset. This sulfate bias may also contribute to the remaining bias in ammonium aerosol. Regional SO_2 emission estimates from the CEDS inventory, used in these simulations, are higher than regional estimates from the other four inventories considered in Figure 2, potentially contributing to this high bias. Unfortunately, satellite measurements of SO_2 are not sensitive enough to appropriately constrain these precursor emissions.

3.5. $PM_{2.5}$ Exposure, Health Assessment, and Source Attribution. The more robust performance of the Modified simulation against the independent observations from aircraft and surface measurements enables a validated estimate of population exposure to ambient aerosol. The resulting annual population-weighted aerosol exposure in India, of 61.4 μg m^{-3} for 2016, is an order of magnitude higher than the recent

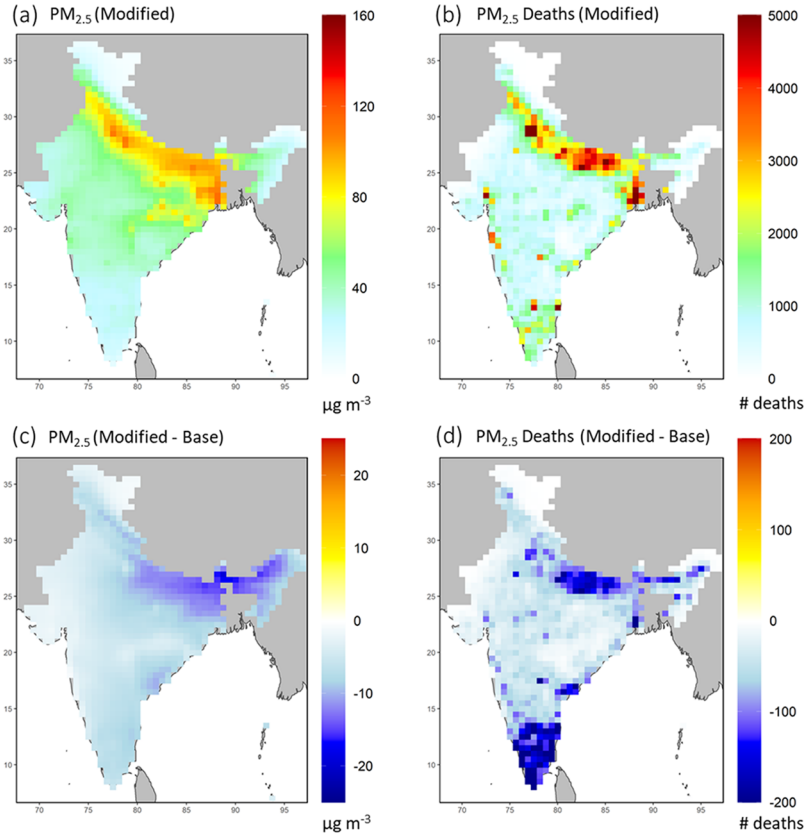

Figure 4. (a) Annual mean $PM_{2.5}$ concentrations and (b) attributable deaths in the Modified simulation. Difference in (c) annual mean $PM_{2.5}$ concentrations and (d) attributable deaths between the Modified and Base simulations. All model outputs are for 2016.

https://doi.org/10.1021/acsearthspacechem.2c00150
ACS Earth Space Chem. 2022, 6, 2432−2445

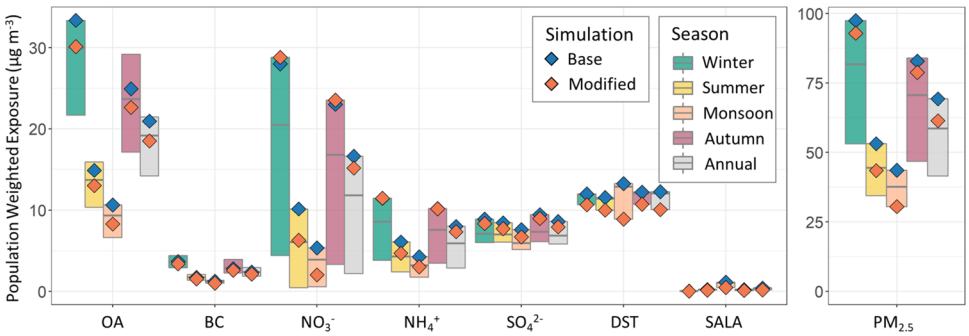

Figure 5. Populated-weighted seasonal and annual exposure to $PM_{2.5}$ and its constituent species for 2016 across different simulations. The bars bound the spread in exposure estimates, and the lines denote the mean values across the different simulations. Seasons are defined as winter (DJF), summer (MAM), monsoon (JJA), and autumn (SON). DST and SALA are fine aerosols from dust and sea salt, respectively.

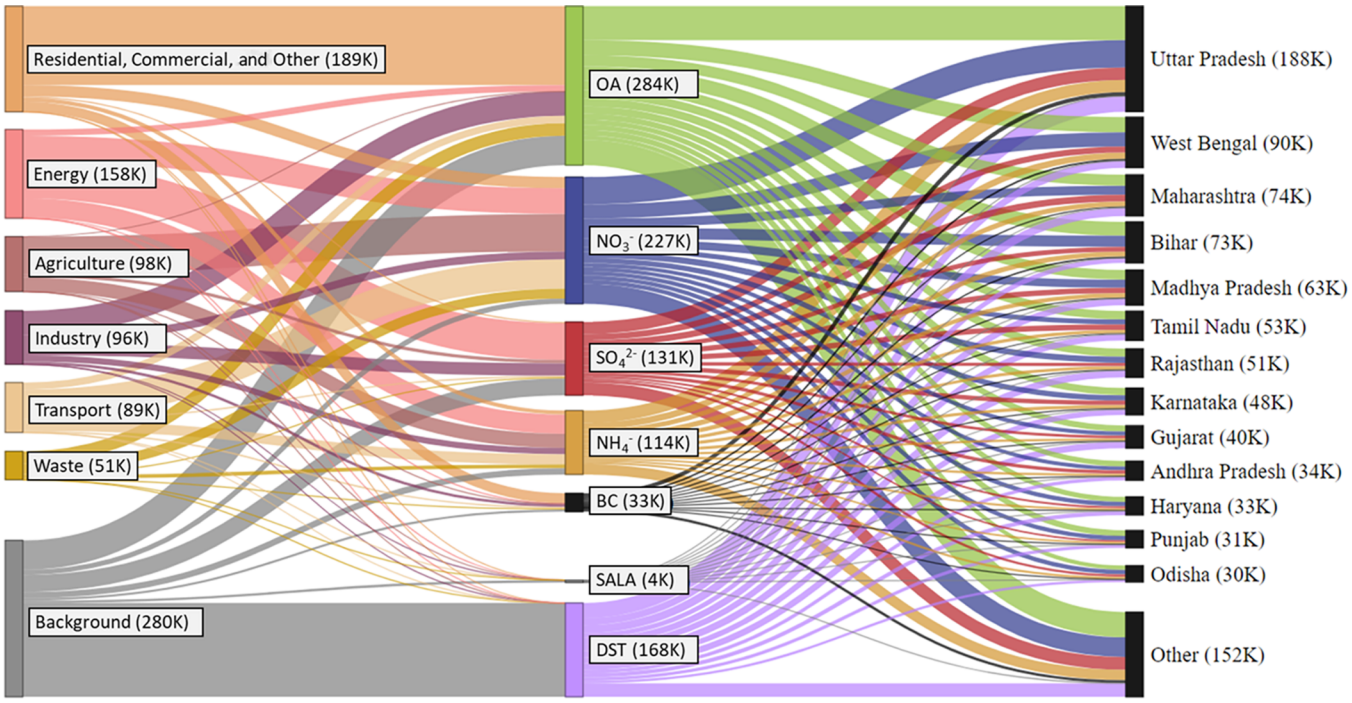

Figure 6. Annual $PM_{2.5}$-related deaths attributable to each source sector, aerosol species, and state in India. States with less than 30,000 annual attributable deaths, and union territories, are lumped under "other". The height of each node and width of each connection correspond to the attributable deaths. Figure S11 provides a complementary illustration of the magnitude of attributable deaths using the Base simulation.

annual exposure guideline of 5 $\mu g\ m^{-3}$ established by the World Health Organization (WHO). There are also large differences in the mean population-weighted aerosol exposure estimates for different states (Figure 4a and Table S1), with the most severe chronic pollution levels manifesting over the northeast states of West Bengal (99 $\mu g\ m^{-3}$), Bihar (96 $\mu g\ m^{-3}$), and Uttar Pradesh (89 $\mu g\ m^{-3}$). Our refined estimate of the national population-weighted annual exposure (of 61.4 $\mu g\ m^{-3}$) is 11% lower than the Base simulation estimate of 69.2 $\mu g\ m^{-3}$. Reductions in simulated aerosol exposure between the Base and Modified simulations are particularly large over the most severely polluted northeast states (Figure 4c), with substantial differences (≥20%) also manifesting across large, more moderately polluted southern states like Andhra Pradesh, Kerala, and Tamil Nadu (Table S1). We note that both the Base and Modified estimates are lower than the population-weighted annual exposure calculations of 92.2, 80.2, and 74.3 $\mu g\ m^{-3}$ from the GBD project,[95] McDuffie et al.,[5] and the GBD MAPS report,[1] respectively, that all use satellite- and surface-derived $PM_{2.5}$ constraints.

Figure 5 shows the range of population-weighted seasonal exposure estimates for different aerosol species when using different emission inventories in India (under the Base configuration). The highest estimated $PM_{2.5}$ exposure is 43–84% greater than the lowest estimated $PM_{2.5}$ exposure, depending on the season. The ranges are most pronounced for the OA, nitrate, and ammonium constituents, which are influenced by primary emissions sources with some of the largest uncertainties,[108] illustrating the urgent need for additional emissions data and constraints on these species and their precursors. The CEDS inventory,[58] used in the Base and Modified simulations, appears near the upper limit for most aerosol species, indicating that regional exposure estimates using this version of the inventory might be viewed as an upper-bound relative to the other inventories tested here. We note that the Modified scheme decreases estimated exposure across all seasons and species, compared to the

https://doi.org/10.1021/acsearthspacechem.2c00150
ACS Earth Space Chem. 2022, 6, 2432–2445

Base simulation. The decrease in total $PM_{2.5}$ exposure is largest in the summer and monsoon seasons.

Using the Modified simulation, we estimate that aerosol pollution accounted for around 961,000 (95th percentile confidence interval: 563,000 | 1,307,000) annual $PM_{2.5}$-attributable deaths in 2016, compared to approximately 1,013,000 (95th percentile confidence interval: 598,000 | 1,370,000) $PM_{2.5}$-attributable deaths estimated using the Base simulation. The estimates are based on an integrated exposure-response model (see the Methods section and the Supporting Information) using age and state-specific baseline mortality rates (BMR), following the India-specific GBD MAPS assessment methodology, which estimated 1.09 million attributable deaths in 2015.[1] (Refer to the Supporting Information for a complementary analysis based on McDuffie et al.[5]). Our estimates are well within previous pollution-attributable mortality calculations that vary between approximately 0.4 and 1.1 million.[1−7] The attributable deaths are highest in polluted states with dense populations (Figures 4b and 6), with the states of Uttar Pradesh (188,000), West Bengal (90,000), Maharashtra (74,000), and Bihar (73,000) experiencing the highest $PM_{2.5}$-attributable deaths. The 11% decrease in population-weighted exposure between the Base and Modified simulations translates to a smaller (5%) relative decrease in estimated attributable deaths due to the non-linear nature of the exposure-response function. This non-linear response also results in a disproportionate decrease in attributable deaths in the southern part of the country when comparing the Base and Modified simulations (Figure 4d).

Developing air quality management policies to address the health burden of aerosol pollution in India requires a robust source-sector analysis. Figure 6 and Figure S9 illustrate the source sensitivities of six different anthropogenic emission sectors as well as natural (including biomass burning) and transboundary sources from the observationally constrained modified simulation. Figure 6 also segments the total $PM_{2.5}$-attributable deaths for each source sector, aerosol species, and state in India. In aggregate, the RCO sector (residential, commercial, and other) that is dominated by residential burning contributes the greatest share (21%), followed by the energy sector (19%), consistent with previous studies.[1−3,5,25,109,110] State-level attributions are shown in Figure S10 and Table S2. The RCO sector dominates across OA and BC, accounting for 50 and 55% of the total contribution for these species, respectively. Emissions from the energy sector account for over 49% of the total sulfate. Energy, transport, and agricultural emissions all play a vital role in controlling nitrate and ammonium concentrations (Table S3). The agricultural contribution to local BC and OA exposure has been shown to be meaningful,[111,112] particularly in the post-harvest months of April to May and October to November, and is likely underestimated in this study since the sectoral emissions of these species in the CEDS inventory are at the low end of the other inventories analyzed (Figure 2). Background levels of $PM_{2.5}$ alone, from natural and transboundary sources, account for a population-weighted exposure of 17.5 $\mu g\ m^{-3}$ (28% of the total estimated exposure), with important implications for determining a policy-relevant background level and setting air quality targets. There are also meaningful differences in the relative sectoral contributions between the Base and Modified simulations (Figures S9 and S11 and Table S2), highlighting the importance of observationally validating model simulations before using them for source-apportionment purposes. In particular, the Base simulation appears to overestimate the contribution of agricultural NH_3 emissions to $PM_{2.5}$ via ammonium nitrate formation, while underestimating the contributions (of NO_x) from energy, transport, and industrial sources.

In aggregate, all the major sectors contribute substantially to aerosol pollution in the region (Figure S9), indicating that air quality management in India must take on a holistic approach to emissions regulations, consistent with previous work.[25] We also note that reductions in emissions from any given source sector would result in a smaller decrease than the total attributable deaths indicated in Figure 6, due to the non-linear exposure-response relationship. There is thus a need for substantial reductions in emissions across multiple sectors before most of the health benefits can be fully realized.

While sensitivity analyses are informative, they rely on accurate sectoral emission estimates within the model inventories. The RCO sector, in particular, consists of a wide range of different emissions that are aggregated together, with large variance in fuel types and usage patterns. There is thus an urgent need for more openly accessible and granular emission estimates. Previous studies have also highlighted emissions from municipal waste burning as currently under-represented in most inventories.[113,114] Similarly, the large seasonal contribution from the burning of agricultural waste in the northern parts of the country[111] is not effectively captured by most inventories and is very likely underestimated in this study. Advances in high-resolution satellite imaging may help capture smaller agricultural (and non-agricultural) fires over the region and improve emission estimates.[115] Recent aerosol measurements have demonstrated the large influence of chloride aerosol in certain Indian cities,[16−19] accounting for up to 16% of the total fine aerosol during seasonal pollution episodes in Delhi.[19] The SWAAMI observations show that, on average, <1% of PM_1 is chloride during the monsoons, indicating that this species is likely not a major contributor to national $PM_{2.5}$ exposure in this season. However, a validated representation of the sources and formation mechanisms for chloride aerosol would likely improve model performance in certain urban regions, particularly during the winter. Similarly, dust emissions are expected to be dominated almost entirely by natural sources, but a more robust inventory of anthropogenic dust and particulate metal emissions (from construction, roads, agriculture, industry, etc.) could be important in certain regions.[63] Prioritizing the study and development of mechanisms that have a disproportionate impact on regional nitrate burdens[116,117] and better constraining the emissions and atmospheric fate of ammonia[118] will also greatly improve aerosol simulations over the Indian subcontinent. Given the large impact of the modified wet deposition scheme in this study, observational constraints on speciated aerosol dry and wet deposition are also urgently needed to validate these important loss processes.

4. CONCLUSIONS

Limitations in the mechanistic fidelity of CTMs, and the large uncertainties in emission estimates, have important implications for climate, epidemiological, and economic research that leverages model output to inform policy decisions. Observationally assessing CTMs prior to applying them to develop policy recommendations is thus of paramount importance. This work demonstrates the value of using compositional information to improve CTM performance and highlights the

https://doi.org/10.1021/acsearthspacechem.2c00150
ACS Earth Space Chem. 2022, 6, 2432−2445

urgent need for more observational constraints on speciated fine particulate matter as well as its gas-phase precursors. Our results suggest that such measurements are needed both at the surface and in the remote troposphere in order to enable a systematic evaluation of regional models, and make them effective diagnostic and predictive tools. This study illustrates how targeted mechanistic adjustments and satellite constraints that are informed by such compositional analyses can substantially improve regional aerosol simulations over India.

We note that there are a few important limitations to this study. The dearth of speciated airborne (and surface) observations in the region limits the ability to robustly validate the model across different seasons. For instance, we are unable to investigate why the modified simulation increases surface $PM_{2.5}$ bias in certain seasons and regions (Figure S7). Additionally, the emissions scaling approach adopted in this study does not leverage a formal inverse modeling approach, which could, particularly when used with seasonally distributed measurements, provide improved insight into geographically and sectorally distributed emissions. The sectoral-apportionment techniques adopted in this study, while consistent with the state-of-the-science, are adversely impacted by the nonlinear response of certain key species like ammonium and nitrate (Tables S2 and S3). As a result, the contribution from certain sectors (like energy and agriculture) could be over- or underestimated in this analysis.

While further model development is necessary to constrain regional $PM_{2.5}$ over India, this study is one of the first to demonstrate how speciated measurements of aerosols (and their precursors) can be used to improve aerosol simulations over the region. As India develops industrially, and as the population ages, we might expect $PM_{2.5}$-attributable mortality to rise meaningfully in the absence of science-based air quality management strategies. Model development and validation efforts that adopt a compositional lens could significantly improve our understanding of aerosol exposure and source-sector sensitivities over the Indian subcontinent and other developing regions, enabling more effective air quality management decisions in these polluted environments.

■ ASSOCIATED CONTENT

Supporting Information

The Supporting Information is available free of charge at https://pubs.acs.org/doi/10.1021/acsearthspacechem.2c00150.

Figure S1. Comparison of MODIS AQUA AOD during the 2016 monsoon period (JJA) compared to Base model AOD during the same time period, as well as additional details. Figure S2. Spatial variance in annual emissions of key pollutants across anthropogenic inventories and pyrogenic inventories. Figure S3. Monthly scaling (in %) of Base national emissions used to adjust emissions for NH_3 and NO_x in the Modified simulation. Figure S4. Seasonally averaged NH_3 and NO_x scaling factors. Figure S5. Vertical profiles for observed and simulated fine aerosol species during the 2016 SWAAMI campaign. Figure S6. Scatter plots comparing observed and simulated seasonal mean fine aerosol concentrations at a number of different surface monitoring sites in India for the year 2017, along with additional details. Figure S7. Comparison of seasonal model skill between the Base and Modified simulations relative to surface $PM_{2.5}$ observations for 2017. Figure S8. Seasonal comparison between ACSM aerosol measurements and model concentrations at a surface monitoring site in Delhi for 2017. Figure S9. Relative sectoral contributions to the total population-weighted annual mean $PM_{2.5}$ exposure for 2016. Figure S10. Dominance of regional $PM_{2.5}$ anthropogenic source sectors using the Modified simulation for 2016. Figure S11. Annual $PM_{2.5}$-related deaths attributable to each source sector, aerosol species, and state in India using the Base simulation. Figure S12. Agro-climatic zones of India (as defined by the Indian Planning Commission). Figure S13. Annually averaged daily satellite NO_2 columns from TROPOMI and OMI. Figure S14. Annual NO_x emissions (2016) over India from lightning NO_x and all NO_x sources. Figure S15. Seasonal comparison of aerosol optical depth (AOD) for 2016 from the Base simulation and retrieved AOD from the MODIS instrument. Figure S16. Seasonal comparison of aerosol optical depth (AOD) for 2016 from the Modified simulation and retrieved AOD from the MODIS instrument. Table S1. Annual mean population-weighted $PM_{2.5}$ exposure across Indian states using the Modified simulation. Table S2. $PM_{2.5}$ source attribution across Indian states using the Modified simulation. Table S3. Aerosol source attribution over India using the Modified simulation. Table S4. List of model simulations analyzed and discussed in the main text. Section S1. Satellite observations. Section S2. Modified simulation and emission masks. Section S3. $PM_{2.5}$-attributable mortality estimates (PDF)

■ AUTHOR INFORMATION

Corresponding Authors

Sidhant J. Pai − *Department of Civil and Environmental Engineering, Massachusetts Institute of Technology, Cambridge, Massachusetts 02139, United States;* orcid.org/0000-0003-3977-4495; Email: sidhantpai@gmail.com

Colette L. Heald − *Department of Civil and Environmental Engineering and Department of Earth, Atmospheric and Planetary Sciences, Massachusetts Institute of Technology, Cambridge, Massachusetts 02139, United States;* orcid.org/0000-0003-2894-5738; Email: heald@mit.edu

Authors

Hugh Coe − *Centre for Atmospheric Science, School of Earth and Environmental Science, University of Manchester, Manchester M13 9PL, UK*

James Brooks − *Centre for Atmospheric Science, School of Earth and Environmental Science, University of Manchester, Manchester M13 9PL, UK*

Mark W. Shephard − *Environment and Climate Change Canada, North York, Ontario M3H 5T4, Canada*

Enrico Dammers − *Environment and Climate Change Canada, North York, Ontario M3H 5T4, Canada; Climate, Air and Sustainability, Netherlands Organization for Applied Scientific Research (TNO), 3584 CB Utrecht, Netherlands*

Joshua S. Apte − *Department of Civil and Environmental Engineering, University of California, Berkeley, California 94720, United States; School of Public Health, University of California, Berkeley, California 94704, United States;* orcid.org/0000-0002-2796-3478

https://doi.org/10.1021/acsearthspacechem.2c00150
ACS Earth Space Chem. 2022, 6, 2432−2445

Gan Luo − *Atmospheric Sciences Research Center, University at Albany, Albany, New York 12226, United States*
Fangqun Yu − *Atmospheric Sciences Research Center, University at Albany, Albany, New York 12226, United States;* orcid.org/0000-0001-8862-4835
Christopher D. Holmes − *Department of Earth, Ocean, and Atmospheric Science, Florida State University, Tallahassee, Florida 32304, United States;* orcid.org/0000-0002-2727-0954
Chandra Venkataraman − *Department of Chemical Engineering, Indian Institute of Technology Bombay, Mumbai, Maharashtra 400076, India; Interdisciplinary Program in Climate Studies, Indian Institute of Technology Bombay, Mumbai, Maharashtra 400076, India;* orcid.org/0000-0002-2280-3360
Pankaj Sadavarte − *Interdisciplinary Program in Climate Studies, Indian Institute of Technology Bombay, Mumbai, Maharashtra 400076, India; Institute for Advanced Sustainability Studies (IASS), 14467 Potsdam, Germany*
Kushal Tibrewal − *Interdisciplinary Program in Climate Studies, Indian Institute of Technology Bombay, Mumbai, Maharashtra 400076, India*

Complete contact information is available at: https://pubs.acs.org/10.1021/acsearthspacechem.2c00150

Author Contributions

C.L.H. and S.J.P. designed the study. S.J.P. modified the code, performed the simulations, and led the analysis. H.C. and J.B. provided aerosol measurements from the SWAAMI campaign. M.W.S. and E.D. provided the CrIS NH_3 data. J.S.A. provided the ACSM observations in Delhi. G.L., F.Y., and C.D.H. contributed to modifications in the GEOS-Chem aerosol simulation. C.V., P.S., and K.T. provided the SMoG-India emission inventory. S.J.P. and C.L.H. wrote the paper with input from the coauthors and the acknowledged individuals.

Notes

The authors declare no competing financial interest.

■ ACKNOWLEDGMENTS

This work was funded by the MIT Tata Center for Technology and Design and the National Science Foundation (AGS 1936642). We would also like to acknowledge Erin E. McDuffie, Viral Shah, Shahzad Gani, and Karen E. Cady-Pereira for their thoughtful comments and feedback on the manuscript. We credit Thakrar et al. 2020 ES&T and Domingo et al. 2021 PNAS for inspiring the graphical presentation style in Figure 6.

■ REFERENCES

(1) GBD MAPS Working Group. Burden of Disease Attributable to Major Air Pollution Sources in India. *Special Report 21;* Health Effects Institute: Boston, MA, 2018; 104.
(2) Conibear, L.; Butt, E. W.; Knote, C.; Arnold, S. R.; Spracklen, D. V. Residential Energy Use Emissions Dominate Health Impacts from Exposure to Ambient Particulate Matter in India. *Nat. Commun.* **2018**, *9*, 617.
(3) David, L. M.; Ravishankara, A. R.; Kodros, J. K.; Pierce, J. R.; Venkataraman, C.; Sadavarte, P. Premature Mortality Due to PM2.5 Over India: Effect of Atmospheric Transport and Anthropogenic Emissions. *GeoHealth* **2019**, *3*, 2−10.
(4) Pandey, A.; Brauer, M.; Cropper, M. L.; Balakrishnan, K.; Mathur, P.; Dey, S.; Turkgulu, B.; Kumar, G. A.; Khare, M.; Beig, G.; Gupta, T.; Krishnankutty, R. P.; Causey, K.; Cohen, A. J.; Bhargava, S.; Aggarwal, A. N.; Agrawal, A.; Awasthi, S.; Bennitt, F.; Bhagwat, S.; Bhanumati, P.; Burkart, K.; Chakma, J. K.; Chiles, T. C.; Chowdhury, S.; Christopher, D. J.; Dey, S.; Fisher, S.; Fraumeni, B.; Fuller, R.; Ghoshal, A. G.; Golechha, M. J.; Gupta, P. C.; Gupta, R.; Gupta, R.; Gupta, S.; Guttikunda, S.; Hanrahan, D.; Harikrishnan, S.; Jeemon, P.; Joshi, T. K.; Kant, R.; Kant, S.; Kaur, T.; Koul, P. A.; Kumar, P.; Kumar, R.; Larson, S. L.; Lodha, R.; Madhipatla, K. K.; Mahesh, P. A.; Malhotra, R.; Managi, S.; Martin, K.; Mathai, M.; Mathew, J. L.; Mehrotra, R.; Mohan, B. V. M.; Mohan, V.; Mukhopadhyay, S.; Mutreja, P.; Naik, N.; Nair, S.; Pandian, J. D.; Pant, P.; Perianayagam, A.; Prabhakaran, D.; Prabhakaran, P.; Rath, G. K.; Ravi, S.; Roy, A.; Sabde, Y. D.; Salvi, S.; Sambandam, S.; Sharma, B.; Sharma, M.; Sharma, S.; Sharma, R. S.; Shrivastava, A.; Singh, S.; Singh, V.; Smith, R.; Stanaway, J. D.; Taghian, G.; Tandon, N.; Thakur, J. S.; Thomas, N. J.; Toteja, G. S.; Varghese, C. M.; Venkataraman, C.; Venugopal, K. N.; Walker, K. D.; Watson, A. Y.; Wozniak, S.; Xavier, D.; Yadama, G. N.; Yadav, G.; Shukla, D. K.; Bekedam, H. J.; Reddy, K. S.; Guleria, R.; Vos, T.; Lim, S. S.; Dandona, R.; Kumar, S.; Kumar, P.; Landrigan, P. J.; Dandona, L. Health and Economic Impact of Air Pollution in the States of India: The Global Burden of Disease Study 2019. *Lancet Planet. Health* **2021**, *5*, e25−e38.
(5) McDuffie, E. E.; Martin, R. V.; Spadaro, J. V.; Burnett, R.; Smith, S. J.; O'Rourke, P.; Hammer, M. S.; van Donkelaar, A.; Bindle, L.; Shah, V.; Jaeglé, L.; Luo, G.; Yu, F.; Adeniran, J. A.; Lin, J.; Brauer, M. Source Sector and Fuel Contributions to Ambient PM2.5 and Attributable Mortality across Multiple Spatial Scales. *Nat. Commun.* **2021**, *12*, 3594.
(6) Cohen, A. J.; Brauer, M.; Burnett, R.; Anderson, H. R.; Frostad, J.; Estep, K.; Balakrishnan, K.; Brunekreef, B.; Dandona, L.; Dandona, R.; Feigin, V.; Freedman, G.; Hubbell, B.; Jobling, A.; Kan, H.; Knibbs, L.; Liu, Y.; Martin, R.; Morawska, L.; Pope, C. A.; Shin, H.; Straif, K.; Shaddick, G.; Thomas, M.; van Dingenen, R.; van Donkelaar, A.; Vos, T.; Murray, C. J. L.; Forouzanfar, M. H. Estimates and 25-Year Trends of the Global Burden of Disease Attributable to Ambient Air Pollution: An Analysis of Data from the Global Burden of Diseases Study 2015. *Lancet* **2017**, *389*, 1907−1918.
(7) World Health Organization. *Ambient Air Pollution: A Global Assessment of Exposure and Burden of Disease*; World Health Organization: 2016.
(8) Burney, J.; Ramanathan, V. Recent Climate and Air Pollution Impacts on Indian Agriculture. *Proc. Natl. Acad. Sci.* **2014**, *111*, 16319−16324.
(9) Schiferl, L. D.; Heald, C. L. Particulate Matter Air Pollution May Offset Ozone Damage to Global Crop Production. *Atmos. Chem. Phys.* **2018**, *18*, 5953−5966.
(10) Guo, L.; Turner, A. G.; Highwood, E. J. Local and Remote Impacts of Aerosol Species on Indian Summer Monsoon Rainfall in a GCM. *J. Clim.* **2016**, *29*, 6937−6955.
(11) Dave, P.; Bhushan, M.; Venkataraman, C. Aerosols Cause Intraseasonal Short-Term Suppression of Indian Monsoon Rainfall. *Sci. Rep.* **2017**, *7*, 17347.
(12) World Bank and Institute for Health Metrics and Evaluation. *The Cost of Air Pollution: Strengthening the Economic Case for Action*; World Bank: Washington, DC, 2016.
(13) Chowdhury, S.; Dey, S.; Smith, K. R. Ambient PM 2.5 Exposure and Expected Premature Mortality to 2100 in India under Climate Change Scenarios. *Nat. Commun.* **2018**, *9*, 318.
(14) Manoj, M. R.; Satheesh, S. K.; Moorthy, K. K.; Gogoi, M. M.; Babu, S. S. Decreasing Trend in Black Carbon Aerosols Over the Indian Region. *Geophys. Res. Lett.* **2019**, *46*, 2903−2910.
(15) Pai, S. J.; Carter, T. S.; Heald, C. L.; Kroll, J. H. Updated World Health Organization Air Quality Guidelines Highlight the Importance of Non-Anthropogenic PM2.5. *Environ. Sci. Technol. Lett.* **2022**, *9*, 501.
(16) Gani, S.; Bhandari, S.; Seraj, S.; Wang, D. S.; Patel, K.; Soni, P.; Arub, Z.; Habib, G.; Hildebrandt Ruiz, L.; Apte, J. S. Submicron Aerosol Composition in the World's Most Polluted Megacity: The

Delhi Aerosol Supersite Study. *Atmos. Chem. Phys.* **2019**, *19*, 6843−6859.
(17) Tobler, A.; Bhattu, D.; Canonaco, F.; Lalchandani, V.; Shukla, A.; Thamban, N. M.; Mishra, S.; Srivastava, A. K.; Bisht, D. S.; Tiwari, S.; Singh, S.; Močnik, G.; Baltensperger, U.; Tripathi, S. N.; Slowik, J. G.; Prévôt, A. S. H. Chemical Characterization of PM2.5 and Source Apportionment of Organic Aerosol in New Delhi, India. *Sci. Total Environ.* **2020**, *745*, No. 140924.
(18) Bhandari, S.; Gani, S.; Patel, K.; Wang, D. S.; Soni, P.; Arub, Z.; Habib, G.; Apte, J. S.; Hildebrandt Ruiz, L. Sources and Atmospheric Dynamics of Organic Aerosol in New Delhi, India: Insights from Receptor Modeling. *Atmos. Chem. Phys.* **2020**, *20*, 735−752.
(19) Gunthe, S. S.; Liu, P.; Panda, U.; Raj, S. S.; Sharma, A.; Darbyshire, E.; Reyes-Villegas, E.; Allan, J.; Chen, Y.; Wang, X.; Song, S.; Pöhlker, M. L.; Shi, L.; Wang, Y.; Kommula, S. M.; Liu, T.; Ravikrishna, R.; McFiggans, G.; Mickley, L. J.; Martin, S. T.; Pöschl, U.; Andreae, M. O.; Coe, H. Enhanced Aerosol Particle Growth Sustained by High Continental Chlorine Emission in India. *Nat. Geosci.* **2021**, 77−84.
(20) Venkataraman, C.; Brauer, M.; Tibrewal, K.; Sadavarte, P.; Ma, Q.; Cohen, A.; Chaliyakunnel, S.; Frostad, J.; Klimont, Z.; Martin, R. V.; Millet, D. B.; Philip, S.; Walker, K.; Wang, S. Source Influence on Emission Pathways and Ambient $PM_{2.5}$ Pollution over India (2015−2050). *Atmos. Chem. Phys.* **2018**, *18*, 8017−8039.
(21) Chowdhury, S.; Dey, S.; Guttikunda, S.; Pillarisetti, A.; Smith, K. R.; Di Girolamo, L. Indian Annual Ambient Air Quality Standard Is Achievable by Completely Mitigating Emissions from Household Sources. *Proc. Natl. Acad. Sci.* **2019**, *116*, 10711−10716.
(22) Guttikunda, S. K.; Nishadh, K. A.; Jawahar, P. Air Pollution Knowledge Assessments (APnA) for 20 Indian Cities. *Urban Clim.* **2019**, *27*, 124−141.
(23) Cropper, M.; Cui, R.; Guttikunda, S.; Hultman, N.; Jawahar, P.; Park, Y.; Yao, X.; Song, X.-P. The Mortality Impacts of Current and Planned Coal-Fired Power Plants in India. *Proc. Natl. Acad. Sci.* **2021**, *118* (), DOI: 10.1073/pnas.2017936118.
(24) Karambelas, A.; Holloway, T.; Kinney, P. L.; Fiore, A. M.; DeFries, R.; Kiesewetter, G.; Heyes, C. Urban versus Rural Health Impacts Attributable to $PM_{2.5}$ and O_3 in Northern India. *Environ. Res. Lett.* **2018**, *13*, No. 064010.
(25) Apte, J. S.; Pant, P. Toward Cleaner Air for a Billion Indians. *Proc. Natl. Acad. Sci.* **2019**, *116*, 10614−10616.
(26) Brauer, M.; Guttikunda, S. K.; Nishad, K. A.; Dey, S.; Tripathi, S. N.; Weagle, C.; Martin, R. V. Examination of Monitoring Approaches for Ambient Air Pollution: A Case Study for India. *Atmos. Environ.* **2019**, *216*, No. 116940.
(27) Pant, P.; Lal, R. M.; Guttikunda, S. K.; Russell, A. G.; Nagpure, A. S.; Ramaswami, A.; Peltier, R. E. Monitoring Particulate Matter in India: Recent Trends and Future Outlook. *Air Qual., Atmos. Health* **2019**, *12*, 45−58.
(28) Bran, S. H.; Srivastava, R. Investigation of PM2.5 Mass Concentration over India Using a Regional Climate Model. *Environ. Pollut.* **2017**, *224*, 484−493.
(29) van Donkelaar, A.; Martin, R. V.; Brauer, M.; Hsu, N. C.; Kahn, R. A.; Levy, R. C.; Lyapustin, A.; Sayer, A. M.; Winker, D. M. Global Estimates of Fine Particulate Matter Using a Combined Geophysical-Statistical Method with Information from Satellites, Models, and Monitors. *Environ. Sci. Technol.* **2016**, *50*, 3762−3772.
(30) Shaddick, G.; Thomas, M. L.; Green, A.; Brauer, M.; van Donkelaar, A.; Burnett, R.; Chang, H. H.; Cohen, A.; Dingenen, R. V.; Dora, C.; Gumy, S.; Liu, Y.; Martin, R.; Waller, L. A.; West, J.; Zidek, J. V.; Prüss-Ustün, A. Data Integration Model for Air Quality: A Hierarchical Approach to the Global Estimation of Exposures to Ambient Air Pollution. *J. R. Stat. Soc.* **2018**, *67*, 231−253.
(31) Hammer, M. S.; van Donkelaar, A.; Li, C.; Lyapustin, A.; Sayer, A. M.; Hsu, N. C.; Levy, R. C.; Garay, M. J.; Kalashnikova, O. V.; Kahn, R. A.; Brauer, M.; Apte, J. S.; Henze, D. K.; Zhang, L.; Zhang, Q.; Ford, B.; Pierce, J. R.; Martin, R. V. Global Estimates and Long-Term Trends of Fine Particulate Matter Concentrations (1998−2018). *Environ. Sci. Technol.* **2020**, *54*, 7879−7890.
(32) Bey, I.; Jacob, D. J.; Yantosca, R. M.; Logan, J. A.; Field, B. D.; Fiore, A. M.; Li, Q.; Liu, H. Y.; Mickley, L. J.; Schultz, M. G. Global Modeling of Tropospheric Chemistry with Assimilated Meteorology: Model Description and Evaluation. *J. Geophys. Res.: Atmos.* **2001**, *106*, 23073−23095.
(33) Philip, S.; Martin, R. V.; Keller, C. A. Sensitivity of Chemistry-Transport Model Simulations to the Duration of Chemical and Transport Operators: A Case Study with GEOS-Chem V10-01. *Geosci. Model Dev.* **2016**, *9*, 1683−1695.
(34) Mao, J.; Paulot, F.; Jacob, D. J.; Cohen, R. C.; Crounse, J. D.; Wennberg, P. O.; Keller, C. A.; Hudman, R. C.; Barkley, M. P.; Horowitz, L. W. Ozone and Organic Nitrates over the Eastern United States: Sensitivity to Isoprene Chemistry. *J. Geophys. Res.: Atmos.* **2013**, *118*, 11,256−11,268.
(35) Travis, K. R.; Jacob, D. J.; Fisher, J. A.; Kim, P. S.; Marais, E. A.; Zhu, L.; Yu, K.; Miller, C. C.; Yantosca, R. M.; Sulprizio, M. P.; Thompson, A. M.; Wennberg, P. O.; Crounse, J. D.; St. Clair, J. M.; Cohen, R. C.; Laughner, J. L.; Dibb, J. E.; Hall, S. R.; Ullmann, K.; Wolfe, G. M.; Pollack, I. B.; Peischl, J.; Neuman, J. A.; Zhou, X. Why Do Models Overestimate Surface Ozone in the Southeast United States? *Atmos. Chem. Phys.* **2016**, *16*, 13561−13577.
(36) Chan Miller, C.; Jacob, D. J.; Marais, E. A.; Yu, K.; Travis, K. R.; Kim, P. S.; Fisher, J. A.; Zhu, L.; Wolfe, G. M.; Hanisco, T. F.; Keutsch, F. N.; Kaiser, J.; Min, K.-E.; Brown, S. S.; Washenfelder, R. A.; González Abad, G.; Chance, K. Glyoxal Yield from Isoprene Oxidation and Relation to Formaldehyde: Chemical Mechanism, Constraints from SENEX Aircraft Observations, and Interpretation of OMI Satellite Data. *Atmos. Chem. Phys.* **2017**, *17*, 8725−8738.
(37) Fischer, E. V.; Jacob, D. J.; Yantosca, R. M.; Sulprizio, M. P.; Millet, D. B.; Mao, J.; Paulot, F.; Singh, H. B.; Roiger, A.; Ries, L.; Talbot, R. W.; Dzepina, K.; Pandey Deolal, S. Atmospheric Peroxyacetyl Nitrate (PAN): A Global Budget and Source Attribution. *Atmos. Chem. Phys.* **2014**, *14*, 2679−2698.
(38) Sherwen, T.; Schmidt, J. A.; Evans, M. J.; Carpenter, L. J.; Großmann, K.; Eastham, S. D.; Jacob, D. J.; Dix, B.; Koenig, T. K.; Sinreich, R.; Ortega, I.; Volkamer, R.; Saiz-Lopez, A.; Prados-Roman, C.; Mahajan, A. S.; Ordóñez, C. Global Impacts of Tropospheric Halogens (Cl, Br, I) on Oxidants and Composition in GEOS-Chem. *Atmos. Chem. Phys.* **2016**, *16*, 12239−12271.
(39) Park, R. J. Natural and Transboundary Pollution Influences on Sulfate-Nitrate-Ammonium Aerosols in the United States: Implications for Policy. *J. Geophys. Res.* **2004**, *109* (), DOI: 10.1029/2003JD004473.
(40) Jaeglé, L.; Quinn, P. K.; Bates, T. S.; Alexander, B.; Lin, J.-T. Global Distribution of Sea Salt Aerosols: New Constraints from in Situ and Remote Sensing Observations. *Atmos. Chem. Phys.* **2011**, *11*, 3137−3157.
(41) Park, R. J.; Jacob, D. J.; Chin, M.; Martin, R. V. Sources of Carbonaceous Aerosols over the United States and Implications for Natural Visibility. *J. Geophys. Res.* **2003**, *108* (), DOI: 10.1029/2002JD003190.
(42) Wang, Q.; Jacob, D. J.; Spackman, J. R.; Perring, A. E.; Schwarz, J. P.; Moteki, N.; Marais, E. A.; Ge, C.; Wang, J.; Barrett, S. R. H. Global Budget and Radiative Forcing of Black Carbon Aerosol: Constraints from Pole-to-Pole (HIPPO) Observations across the Pacific. *J. Geophys. Res.: Atmos.* **2014**, *119*, 195−206.
(43) Pai, S. J.; Heald, C. L.; Pierce, J. R.; Farina, S. C.; Marais, E. A.; Jimenez, J. L.; Campuzano-Jost, P.; Nault, B. A.; Middlebrook, A. M.; Coe, H.; Shilling, J. E.; Bahreini, R.; Dingle, J. H.; Vu, K. An Evaluation of Global Organic Aerosol Schemes Using Airborne Observations. *Atmos. Chem. Phys.* **2020**, *20*, 2637−2665.
(44) Fairlie, D. T.; Jacob, D. J.; Park, R. J. The Impact of Transpacific Transport of Mineral Dust in the United States. *Atmos. Environ.* **2007**, *41*, 1251−1266.
(45) Ridley, D. A.; Heald, C. L.; Ford, B. North African Dust Export and Deposition: A Satellite and Model Perspective. *J. Geophys. Res.: Atmos.* **2012**, *117* (), DOI: 10.1029/2011JD016794.
(46) Fountoukis, C.; Nenes, A. ISORROPIA II: A Computationally Efficient Thermodynamic Equilibrium Model for K+−Ca2+−Mg2+−

NH4+−Na+−SO24−−NO−3 −Cl−−H2O Aerosols. *Atmos. Chem. Phys.* **2007**, *7*, 4639−4659.
(47) Chin, M.; Ginoux, P.; Kinne, S.; Torres, O.; Holben, B. N.; Duncan, B. N.; Martin, R. V.; Logan, J. A.; Higurashi, A.; Nakajima, T. Tropospheric Aerosol Optical Thickness from the GOCART Model and Comparisons with Satellite and Sun Photometer Measurements. *J. Atmos. Sci.* **2002**, *59*, 461−483.
(48) Cooke, W. F.; Liousse, C.; Cachier, H.; Feichter, J. Construction of a 1° × 1° Fossil Fuel Emission Data Set for Carbonaceous Aerosol and Implementation and Radiative Impact in the ECHAM4 Model. *J. Geophys. Res.: Atmos.* **1999**, *104*, 22137−22162.
(49) Latimer, R. N. C.; Martin, R. V. Interpretation of Measured Aerosol Mass Scattering Efficiency over North America Using a Chemical Transport Model. *Atmos. Chem. Phys.* **2019**, *19*, 2635−2653.
(50) Wesely, M. L. Parameterization of Surface Resistances to Gaseous Dry Deposition in Regional-Scale Numerical Models. *Atmos. Environ. (1967)* **1989**, *23*, 1293−1304.
(51) Zhang, L.; Gong, S.; Padro, J.; Barrie, L. A Size-Segregated Particle Dry Deposition Scheme for an Atmospheric Aerosol Module. *Atmos. Environ.* **2001**, *35*, 549−560.
(52) Amos, H. M.; Jacob, D. J.; Holmes, C. D.; Fisher, J. A.; Wang, Q.; Yantosca, R. M.; Corbitt, E. S.; Galarneau, E.; Rutter, A. P.; Gustin, M. S.; Steffen, A.; Schauer, J. J.; Graydon, J. A.; Louis, V. L. S.; Talbot, R. W.; Edgerton, E. S.; Zhang, Y.; Sunderland, E. M. Gas-Particle Partitioning of Atmospheric Hg(II) and Its Effect on Global Mercury Deposition. *Atmos. Chem. Phys.* **2012**, *12*, 591−603.
(53) Jacob, D. J.; Liu, H.; Mari, C.; Yantosca, R. M. *Harvard Wet Deposition Scheme for GMI*; Harvard University Atmospheric Chemistry Modeling Group: 2000, 6.
(54) Liu, H.; Jacob, D. J.; Bey, I.; Yantosca, R. M. Constraints from ^{210}Pb and ^{7}Be on Wet Deposition and Transport in a Global Three-Dimensional Chemical Tracer Model Driven by Assimilated Meteorological Fields. *J. Geophys. Res.: Atmos.* **2001**, *106*, 12109−12128.
(55) Rastigejev, Y.; Park, R.; Brenner, M. P.; Jacob, D. J. Resolving Intercontinental Pollution Plumes in Global Models of Atmospheric Transport. *J. Geophys. Res.: Atmos.* **2010**, *115* (), DOI: 10.1029/2009JD012568.
(56) GEOS-Chem Aerosols Working Group. *Particulate matter in GEOS-Chem*. http://wiki.seas.harvard.edu/geos-chem/index.php/Particulate_matter_in_GEOS-Chem (accessed 2021-02-24).
(57) Central Pollution Control Board. Guidelines for Real Time Sampling & Analyses. *Guidelines for the Measurement of Ambient Air Pollutants*; CENTRAL POLLUTION CONTROL BOARD: 2012, *2*, 62.
(58) Hoesly, R. M.; Smith, S. J.; Feng, L.; Klimont, Z.; Janssens-Maenhout, G.; Pitkanen, T.; Seibert, J. J.; Vu, L.; Andres, R. J.; Bolt, R. M.; Bond, T. C.; Dawidowski, L.; Kholod, N.; Kurokawa, J.; Li, M.; Liu, L.; Lu, Z.; Moura, M. C. P.; O'Rourke, P. R.; Zhang, Q. Historical (1750−2014) Anthropogenic Emissions of Reactive Gases and Aerosols from the Community Emissions Data System (CEDS). *Geosci. Model Dev.* **2018**, *11*, 369−408.
(59) Murray, L. T.; Jacob, D. J.; Logan, J. A.; Hudman, R. C.; Koshak, W. J. Optimized Regional and Interannual Variability of Lightning in a Global Chemical Transport Model Constrained by LIS/OTD Satellite Data. *J. Geophys. Res.: Atmos.* **2012**, *117* (), DOI: 10.1029/2012JD017934.
(60) Ott, L. E.; Pickering, K. E.; Stenchikov, G. L.; Allen, D. J.; DeCaria, A. J.; Ridley, B.; Lin, R.-F.; Lang, S.; Tao, W.-K. Production of Lightning NO_x and Its Vertical Distribution Calculated from Three-Dimensional Cloud-Scale Chemical Transport Model Simulations. *J. Geophys. Res.: Atmos.* **2010**, *115* (), DOI: 10.1029/2009JD011880.
(61) Hudman, R. C.; Moore, N. E.; Mebust, A. K.; Martin, R. V.; Russell, A. R.; Valin, L. C.; Cohen, R. C. Steps towards a Mechanistic Model of Global Soil Nitric Oxide Emissions: Implementation and Space Based-Constraints. *Atmos. Chem. Phys.* **2012**, *12*, 7779−7795.
(62) Holmes, C. D.; Prather, M. J.; Vinken, G. C. M. The Climate Impact of Ship NO_x Emissions: An Improved Estimate Accounting for Plume Chemistry. *Atmos. Chem. Phys.* **2014**, *14*, 6801−6812.
(63) Philip, S.; Martin, R. V.; Snider, G.; Weagle, C. L.; van Donkelaar, A.; Brauer, M.; Henze, D. K.; Klimont, Z.; Venkataraman, C.; Guttikunda, S. K.; Zhang, Q. Anthropogenic Fugitive, Combustion and Industrial Dust Is a Significant, Underrepresented Fine Particulate Matter Source in Global Atmospheric Models. *Environ. Res. Lett.* **2017**, *12*, No. 044018.
(64) Guenther, A. B.; Jiang, X.; Heald, C. L.; Sakulyanontvittaya, T.; Duhl, T.; Emmons, L. K.; Wang, X. The Model of Emissions of Gases and Aerosols from Nature Version 2.1 (MEGAN2.1): An Extended and Updated Framework for Modeling Biogenic Emissions. *Geosci. Model Dev.* **2012**, *5*, 1471−1492.
(65) van der Werf, G. R.; Randerson, J. T.; Giglio, L.; van Leeuwen, T. T.; Chen, Y.; Rogers, B. M.; Mu, M.; van Marle, M. J. E.; Morton, D. C.; Collatz, G. J.; Yokelson, R. J.; Kasibhatla, P. S. Global Fire Emission estimates during 1997−2016. *Earth Syst. Sci. Data* **2017**, *9*, 697−720.
(66) Li, M.; Zhang, Q.; Kurokawa, J.; Woo, J.-H.; He, K.; Lu, Z.; Ohara, T.; Song, Y.; Streets, D. G.; Carmichael, G. R.; Cheng, Y.; Hong, C.; Huo, H.; Jiang, X.; Kang, S.; Liu, F.; Su, H.; Zheng, B. MIX: A Mosaic Asian Anthropogenic Emission Inventory under the International Collaboration Framework of the MICS-Asia and HTAP. *Atmos. Chem. Phys.* **2017**, *17*, 935−963.
(67) Pandey, A.; Sadavarte, P.; Rao, A. B.; Venkataraman, C. Trends in Multi-Pollutant Emissions from a Technology-Linked Inventory for India: II. Residential, Agricultural and Informal Industry Sectors. *Atmos. Environ.* **2014**, *99*, 341−352.
(68) Sadavarte, P.; Venkataraman, C. Trends in Multi-Pollutant Emissions from a Technology-Linked Inventory for India: I. *Industry and Transport Sectors*. *Atmos. Environ.* **2014**, *99*, 353−364.
(69) International Institute for Applied Systems Analysis. *ECLIPSE V5a Global Emissions*. https://iiasa.ac.at/web/home/research/researchPrograms/air/ECLIPSEv5a.html (accessed 2021-03-03).
(70) European Commission. *Emissions Database for Global Atmospheric Research v4.3.1 (January 2016)*. https://edgar.jrc.ec.europa.eu/overview.php?v=431 (accessed 2021-03-03).
(71) Kaiser, J. W.; Heil, A.; Andreae, M. O.; Benedetti, A.; Chubarova, N.; Jones, L.; Morcrette, J.-J.; Razinger, M.; Schultz, M. G.; Suttie, M.; van der Werf, G. R. Biomass Burning Emission estimated with a Global Fire Assimilation System Based on Observed Fire Radiative Power. *Biogeosciences* **2012**, *9*, 527−554.
(72) Wiedinmyer, C.; Akagi, S. K.; Yokelson, R. J.; Emmons, L. K.; Al-Saadi, J. A.; Orlando, J. J.; Soja, A. J. The Fire INventory from NCAR (FINN): A High Resolution Global Model to Estimate the Emissions from Open Burning. *Geosci. Model Dev.* **2011**, *4*, 625−641.
(73) Koster, R. D.; Darmenov, A. S.; Da Silva, A. M. The Quick Fire Emissions Dataset (QFED): Documentation of Versions 2.1, 2.2 and 2.4. NASA/TM-2015-104606 2015.
(74) Brooks, J.; Allan, J. D.; Williams, P. I.; Liu, D.; Fox, C.; Haywood, J.; Langridge, J. M.; Highwood, E. J.; Kompalli, S. K.; O'Sullivan, D.; Babu, S. S.; Satheesh, S. K.; Turner, A. G.; Coe, H. Vertical and Horizontal Distribution of Submicron Aerosol Chemical Composition and Physical Characteristics across Northern India during Pre-Monsoon and Monsoon Seasons. *Atmos. Chem. Phys.* **2019**, *19*, 5615−5634.
(75) DeCarlo, P. F.; Kimmel, J. R.; Trimborn, A.; Northway, M. J.; Jayne, J. T.; Aiken, A. C.; Gonin, M.; Fuhrer, K.; Horvath, T.; Docherty, K. S.; Worsnop, D. R.; Jimenez, J. L. Field-Deployable, High-Resolution, Time-of-Flight Aerosol Mass Spectrometer. *Anal. Chem.* **2006**, *78*, 8281−8289.
(76) Bahreini, R.; Ervens, B.; Middlebrook, A. M.; Warneke, C.; de Gouw, J. A.; DeCarlo, P. F.; Jimenez, J. L.; Brock, C. A.; Neuman, J. A.; Ryerson, T. B.; Stark, H.; Atlas, E.; Brioude, J.; Fried, A.; Holloway, J. S.; Peischl, J.; Richter, D.; Walega, J.; Weibring, P.; Wollny, A. G.; Fehsenfeld, F. C. Organic Aerosol Formation in Urban and Industrial Plumes near Houston and Dallas, Texas. *J. Geophys. Res.* **2009**, *114*, DOI: 10.1029/2008JD011493.

(77) Stephens, M.; Turner, N.; Sandberg, J. Particle Identification by Laser-Induced Incandescence in a Solid-State Laser Cavity. *Appl. Opt.* **2003**, *42*, 3726.
(78) Sayer, A. M.; Munchak, L. A.; Hsu, N. C.; Levy, R. C.; Bettenhausen, C.; Jeong, M.-J. MODIS Collection 6 Aerosol Products: Comparison between Aqua's e-Deep Blue, Dark Target, and "Merged" Data Sets, and Usage Recommendations. *J. Geophys. Res.: Atmos.* **2014**, *119*, 13,965−13,989.
(79) Winker, D. M.; Vaughan, M. A.; Omar, A.; Hu, Y.; Powell, K. A.; Liu, Z.; Hunt, W. H.; Young, S. A. Overview of the CALIPSO Mission and CALIOP Data Processing Algorithms. *J. Atmos. Ocean. Technol.* **2009**, *26*, 2310−2323.
(80) NASA EarthData. *CALIPSO Lidar Level 3 Aerosol Profiles, Cloud Free Data, Standard V3−00*. https://asdc.larc.nasa.gov/project/CALIPSO/CAL_LID_L3_APro_CloudFree-Standard-V3-00_V3-00 (accessed 2021-08-19).
(81) Shephard, M. W.; Cady-Pereira, K. E. Cross-Track Infrared Sounder (CrIS) Satellite Observations of Tropospheric Ammonia. *Atmos. Meas. Tech.* **2015**, *8*, 1323−1336.
(82) Dammers, E.; Shephard, M. W.; Palm, M.; Cady-Pereira, K.; Capps, S.; Lutsch, E.; Strong, K.; Hannigan, J. W.; Ortega, I.; Toon, G. C.; Stremme, W.; Grutter, M.; Jones, N.; Smale, D.; Siemons, J.; Hrpcek, K.; Tremblay, D.; Schaap, M.; Notholt, J.; Erisman, J. W. Validation of the CrIS Fast Physical NH3 Retrieval with Ground-Based FTIR. *Atmos. Meas. Tech.* **2017**, *10*, 2645−2667.
(83) Shephard, M. W.; Dammers, E.; Cady-Pereira, K. E.; Kharol, S. K.; Thompson, J.; Gainariu-Matz, Y.; Zhang, J.; McLinden, C. A.; Kovachik, A.; Moran, M.; Bittman, S.; Sioris, C. E.; Griffin, D.; Alvarado, M. J.; Lonsdale, C.; Savic-Jovcic, V.; Zheng, Q. Ammonia Measurements from Space with the Cross-Track Infrared Sounder: Characteristics and Applications. *Atmos. Chem. Phys.* **2020**, *20*, 2277−2302.
(84) Veefkind, J. P.; Aben, I.; McMullan, K.; Förster, H.; de Vries, J.; Otter, G.; Claas, J.; Eskes, H. J.; de Haan, J. F.; Kleipool, Q.; van Weele, M.; Hasekamp, O.; Hoogeveen, R.; Landgraf, J.; Snel, R.; Tol, P.; Ingmann, P.; Voors, R.; Kruizinga, B.; Vink, R.; Visser, H.; Levelt, P. F. TROPOMI on the ESA Sentinel-5 Precursor: A GMES Mission for Global Observations of the Atmospheric Composition for Climate, Air Quality and Ozone Layer Applications. *Remote Sens. Environ.* **2012**, *120*, 70−83.
(85) Griffin, D.; Zhao, X.; McLinden, C. A.; Boersma, F.; Bourassa, A.; Dammers, E.; Degenstein, D.; Eskes, H.; Fehr, L.; Fioletov, V.; Hayden, K.; Kharol, S. K.; Li, S.-M.; Makar, P.; Martin, R. V.; Mihele, C.; Mittermeier, R. L.; Krotkov, N.; Sneep, M.; Lamsal, L. N.; ter Linden, M.; van Geffen, J.; Veefkind, P.; Wolde, M. High-Resolution Mapping of Nitrogen Dioxide With TROPOMI: First Results and Validation Over the Canadian Oil Sands. *Geophys. Res. Lett.* **2019**, *46*, 1049−1060.
(86) OpenAQ. *Air Quality Data Archive*. OpenAQ. https://openaq.org/ (accessed 2019-03-01).
(87) Central Pollution Control Board. *Continuous Ambient Air Quality Monitoring Stations*. https://app.cpcbccr.com/ccr/#/caaqm-dashboard-all/caaqm-landing (accessed 2021-08-18).
(88) US Department of State. *AirNow Portal*. https://www.airnow.gov/international/us-embassies-and-consulates (accessed 2021-08-18).
(89) Vaughn, D. L. *Standard Operating Procedure for the Continuous Measurement of Particulate Matter*. Met One BAM-1020 PM2.5 Federal Equivalent Method EQPM-0308-170, Sonoma Technology, Inc.: 2009.
(90) Hanley, T.; Reff, A. *Assessment of PM2.5 FEMs Compared to Collocated FRMs*; United States Environmental Protection Agency: 2011.
(91) Gani, S.; Bhandari, S.; Seraj, S.; Wang, D. S.; Patel, K.; Soni, P.; Arub, Z.; Habib, G.; Hildebrandt Ruiz, L.; Apte, J. Submicron Aerosol Composition in the World's Most Polluted Megacity: The Delhi Aerosol Supersite Study. *Atmos. Chem. Phys.* **2020**, DOI: 10.18738/T8/9L33CI.
(92) Ng, N. L.; Herndon, S. C.; Trimborn, A.; Canagaratna, M. R.; Croteau, P. L.; Onasch, T. B.; Sueper, D.; Worsnop, D. R.; Zhang, Q.; Sun, Y. L.; Jayne, J. T. An Aerosol Chemical Speciation Monitor (ACSM) for Routine Monitoring of the Composition and Mass Concentrations of Ambient Aerosol. *Aerosol Sci. Technol.* **2011**, *45*, 780−794.
(93) Burnett, R. T.; Pope, C. A., III; Ezzati, M.; Olives, C.; Lim, S. S.; Mehta, S.; Shin, H. H.; Singh, G.; Hubbell, B.; Brauer, M.; Ross Anderson, H.; Smith, K. R.; Balmes, J. R.; Bruce, N. G.; Kan, H.; Laden, F.; Prüss-Ustün, A.; Turner, M. C.; Gapstur, S. M.; Ryan Diver, W.; Cohen, A. An Integrated Risk Function for Estimating the Global Burden of Disease Attributable to Ambient Fine Particulate Matter Exposure. *Environ. Health Perspect.* **2014**, *122*, 397−403.
(94) Lelieveld, J.; Haines, A.; Pozzer, A. Age-Dependent Health Risk from Ambient Air Pollution: A Modelling and Data Analysis of Childhood Mortality in Middle-Income and Low-Income Countries. *Lancet Planet. Health* **2018**, *2*, e292−e300.
(95) Health Effects Institute. *Health Effects Institute State of Global Air 2018*, 2018.
(96) *Center for International Earth Science Information Network (CIESIN)*; Columbia University: Gridded Population of the World, Version 4 (GPWv4), Revision 11 Data Sets, 2018.
(97) Office of the Registrar General and Census Commissioner. *Census of India Website*. https://censusindia.gov.in/2011-common/censusdata2011.html (accessed 2021-03-01).
(98) The World Bank Group. *India Population, Total*. https://data.worldbank.org/indicator/SP.POP.TOTL?locations=IN (accessed 2021-07-07).
(99) Carter, T. S.; Heald, C. L.; Jimenez, J. L.; Campuzano-Jost, P.; Kondo, Y.; Moteki, N.; Schwarz, J. P.; Wiedinmyer, C.; Darmenov, A. S.; da Silva, A. M.; Kaiser, J. W. How Emissions Uncertainty Influences the Distribution and Radiative Impacts of Smoke from Fires in North America. *Atmos. Chem. Phys.* **2020**, *20*, 2073−2097.
(100) Saikawa, E.; Trail, M.; Zhong, M.; Wu, Q.; Young, C. L.; Janssens-Maenhout, G.; Klimont, Z.; Wagner, F.; Kurokawa, J.; Nagpure, A. S.; Gurjar, B. R. Uncertainties in Emissions Estimates of Greenhouse Gases and Air Pollutants in India and Their Impacts on Regional Air Quality. *Environ. Res. Lett.* **2017**, *12*, No. 065002.
(101) Shah, V.; Jaeglé, L.; Thornton, J. A.; Lopez-Hilfiker, F. D.; Lee, B. H.; Schroder, J. C.; Campuzano-Jost, P.; Jimenez, J. L.; Guo, H.; Sullivan, A. P.; Weber, R. J.; Green, J. R.; Fiddler, M. N.; Bililign, S.; Campos, T. L.; Stell, M.; Weinheimer, A. J.; Montzka, D. D.; Brown, S. S. Chemical Feedbacks Weaken the Wintertime Response of Particulate Sulfate and Nitrate to Emissions Reductions over the Eastern United States. *Proc. Natl. Acad. Sci.* **2018**, *115*, 8110−8115.
(102) McDuffie, E. E.; Fibiger, D. L.; Dubé, W. P.; Hilfiker, F. L.; Lee, B. H.; Jaeglé, L.; Guo, H.; Weber, R. J.; Reeves, J. M.; Weinheimer, A. J.; Schroder, J. C.; Campuzano-Jost, P.; Jimenez, J. L.; Dibb, J. E.; Veres, P.; Ebben, C.; Sparks, T. L.; Wooldridge, P. J.; Cohen, R. C.; Campos, T.; Hall, S. R.; Ullmann, K.; Roberts, J. M.; Thornton, J. A.; Brown, S. S. ClNO2 Yields From Aircraft Measurements During the 2015 WINTER Campaign and Critical Evaluation of the Current Parameterization. *J. Geophys. Res.: Atmos.* **2018**, *123*, 994−13,015.
(103) McDuffie, E. E.; Fibiger, D. L.; Dubé, W. P.; Lopez-Hilfiker, F.; Lee, B. H.; Thornton, J. A.; Shah, V.; Jaeglé, L.; Guo, H.; Weber, R. J.; Michael Reeves, J.; Weinheimer, A. J.; Schroder, J. C.; Campuzano-Jost, P.; Jimenez, J. L.; Dibb, J. E.; Veres, P.; Ebben, C.; Sparks, T. L.; Wooldridge, P. J.; Cohen, R. C.; Hornbrook, R. S.; Apel, E. C.; Campos, T.; Hall, S. R.; Ullmann, K.; Brown, S. S. Heterogeneous N_2O_5 Uptake During Winter: Aircraft Measurements During the 2015 WINTER Campaign and Critical Evaluation of Current Parameterizations. *J. Geophys. Res.: Atmos.* **2018**, *123*, 4345−4372.
(104) Fairlie, T. D.; Jacob, D. J.; Dibb, J. E.; Alexander, B.; Avery, M. A.; van Donkelaar, A.; Zhang, L. Impact of Mineral Dust on Nitrate, Sulfate, and Ozone in Transpacific Asian Pollution Plumes. *Atmos. Chem. Phys.* **2010**, *10*, 3999−4012.

(105) Luo, G.; Yu, F.; Schwab, J. Revised Treatment of Wet Scavenging Processes Dramatically Improves GEOS-Chem 12.0.0 Simulations of Surface Nitric Acid, Nitrate, and Ammonium over the United States. *Geosci. Model Dev.* **2019**, *12*, 3439−3447.
(106) Choi, J.; Henze, D. K.; Cao, H.; Nowlan, C. R.; González Abad, G.; Kwon, H.-A.; Lee, H.-M.; Oak, Y. J.; Park, R. J.; Bates, K. H.; Maasakkers, J. D.; Wisthaler, A.; Weinheimer, A. J. An Inversion Framework for Optimizing Non-Methane VOC Emissions Using Remote Sensing and Airborne Observations in Northeast Asia During the KORUS-AQ Field Campaign. *J. Geophys. Res.: Atmos.* **2022**, *127*, No. e2021JD035844.
(107) Verhoelst, T.; Compernolle, S.; Pinardi, G.; Lambert, J.-C.; Eskes, H. J.; Eichmann, K.-U.; Fjæraa, A. M.; Granville, J.; Niemeijer, S.; Cede, A.; Tiefengraber, M.; Hendrick, F.; Pazmiño, A.; Bais, A.; Bazureau, A.; Boersma, K. F.; Bognar, K.; Dehn, A.; Donner, S.; Elokhov, A.; Gebetsberger, M.; Goutail, F.; Grutter de la Mora, M.; Gruzdev, A.; Gratsea, M.; Hansen, G. H.; Irie, H.; Jepsen, N.; Kanaya, Y.; Karagkiozidis, D.; Kivi, R.; Kreher, K.; Levelt, P. F.; Liu, C.; Müller, M.; Navarro Comas, M.; Piters, A. J. M.; Pommereau, J.-P.; Portafaix, T.; Prados-Roman, C.; Puentedura, O.; Querel, R.; Remmers, J.; Richter, A.; Rimmer, J.; Rivera Cárdenas, C.; Saavedra de Miguel, L.; Sinyakov, V. P.; Stremme, W.; Strong, K.; Van Roozendael, M.; Veefkind, J. P.; Wagner, T.; Wittrock, F.; Yela González, M.; Zehner, C. Ground-Based Validation of the Copernicus Sentinel-5P TROPOMI NO_2 Measurements with the NDACC ZSL-DOAS, MAX-DOAS and Pandonia Global Networks. *Atmos. Meas. Tech.* **2021**, *14*, 481−510.
(108) McDuffie, E. E.; Smith, S. J.; O'Rourke, P.; Tibrewal, K.; Venkataraman, C.; Marais, E. A.; Zheng, B.; Crippa, M.; Brauer, M.; Martin, R. V. A Global Anthropogenic Emission Inventory of Atmospheric Pollutants from Sector- and Fuel-Specific Sources (1970−2017): An Application of the Community Emissions Data System (CEDS). *Earth Syst. Sci. Data* **2020**, *12*, 3413−3442.
(109) Lelieveld, J.; Evans, J. S.; Fnais, M.; Giannadaki, D.; Pozzer, A. The Contribution of Outdoor Air Pollution Sources to Premature Mortality on a Global Scale. *Nature* **2015**, *525*, 367−371.
(110) Guo, H.; Kota, S. H.; Chen, K.; Sahu, S. K.; Hu, J.; Ying, Q.; Wang, Y.; Zhang, H. Source Contributions and Potential Reductions to Health Effects of Particulate Matter in India. *Atmos. Chem. Phys.* **2018**, *18*, 15219−15229.
(111) Liu, T.; Marlier, M. E.; DeFries, R. S.; Westervelt, D. M.; Xia, K. R.; Fiore, A. M.; Mickley, L. J.; Cusworth, D. H.; Milly, G. Seasonal Impact of Regional Outdoor Biomass Burning on Air Pollution in Three Indian Cities: Delhi, Bengaluru, and Pune. *Atmos. Environ.* **2018**, *172*, 83−92.
(112) Kulkarni, S. H.; Ghude, S. D.; Jena, C.; Karumuri, R. K.; Sinha, B.; Sinha, V.; Kumar, R.; Soni, V. K.; Khare, M. How Much Does Large-Scale Crop Residue Burning Affect the Air Quality in Delhi? *Environ. Sci. Technol.* **2020**, *54*, 4790−4799.
(113) Sharma, G.; Sinha, B.; Pallavi; Hakkim, H.; Chandra, B. P.; Kumar, A.; Sinha, V. Gridded Emissions of CO, NO_x, SO_2, CO_2, NH_3, HCl, CH_4, $PM_{2.5}$, PM_{10}, BC, and NMVOC from Open Municipal Waste Burning in India. *Environ. Sci. Technol.* **2019**, *53*, 4765−4774.
(114) Nagpure, A. S.; Ramaswami, A.; Russell, A. Characterizing the Spatial and Temporal Patterns of Open Burning of Municipal Solid Waste (MSW) in Indian Cities. *Environ. Sci. Technol.* **2015**, *49*, 12904−12912.
(115) Ramo, R.; Roteta, E.; Bistinas, I.; van Wees, D.; Bastarrika, A.; Chuvieco, E.; van der Werf, G. R. African Burned Area and Fire Carbon Emissions Are Strongly Impacted by Small Fires Undetected by Coarse Resolution Satellite Data. *Proc. Natl. Acad. Sci.* **2021**, *118* (), DOI: 10.1073/pnas.2011160118.
(116) Holmes, C. D.; Bertram, T. H.; Confer, K. L.; Graham, K. A.; Ronan, A. C.; Wirks, C. K.; Shah, V. The Role of Clouds in the Tropospheric NOx Cycle: A New Modeling Approach for Cloud Chemistry and Its Global Implications. *Geophys. Res. Lett.* **2019**, *46*, 4980−4990.
(117) Chan, Y.-C.; Evans, M. J.; He, P.; Holmes, C. D.; Jaeglé, L.; Kasibhatla, P.; Liu, X.-Y.; Sherwen, T.; Thornton, J. A.; Wang, X.; Xie, Z.; Zhai, S.; Alexander, B. Heterogeneous Nitrate Production Mechanisms in Intense Haze Events in the North China Plain. *J. Geophys. Res.: Atmos.* **2021**, *126*, No. e2021JD034688.
(118) Pai, S. J.; Heald, C. L.; Murphy, J. G. Exploring the Global Importance of Atmospheric Ammonia Oxidation. *ACS Earth Space Chem.* **2021**, *5*, 1674−1685.